JGR Oceans

RESEARCH ARTICLE
10.1029/2021JC017718

Special Section:
Uncovering the hidden links between dynamics, chemical, biogeochemical and biological processes under the changing Arctic

Spatial Distributions of Riverine and Marine Dissolved Organic Carbon in the Western Arctic Ocean: Results From the 2018 Korean Expedition

Jinyoung Jung[1], Youngju Lee[1], Kyoung-Ho Cho[1], Eun Jin Yang[1], and Sung-Ho Kang[1]

[1]Division of Polar Ocean Sciences, Korea Polar Research Institute, Incheon, Republic of Korea

Abstract Seasonal primary production and river discharge increases in the Arctic Ocean exert a significant influence on the dissolved organic carbon (DOC) cycle. To improve our knowledge of the spatial heterogeneity of DOC source and concentration in the rapidly changing Arctic Ocean, we investigated the distributions of riverine and marine DOC in the western Arctic Ocean during the summer of 2018. Although the surface bulk DOC concentration indicated no clear distinction in its distribution between the Chukchi Borderland (CBL)/northern Chukchi Sea (NCS) and East Siberian Sea (ESS)/Mendeleyev Ridge (MR) regions, the estimated riverine DOC concentration (28 ± 4.2 μM C) and its contribution (40 ± 5.7%) in the surface layer of the CBL/NCS region were higher than those (19 ± 5.6 μM C and 26 ± 8.5%) in the ESS/MR region, which was attributed to the accumulation of freshwater, strong stratification, and a longer residence time in the CBL/NCS region. In contrast, although marine DOC was the dominant DOC component in both the CBL/NCS and ESS/MR regions, the higher marine DOC concentration (54 ± 8.1 μM C) and its contribution (73 ± 8.2%) in the East Siberian shelf/slope region were consistent with high bacterial abundance, which was associated with extremely high surface phytoplankton blooms sustained by nutrient supply from the deep layer, suggesting that the supply of bioavailable DOC resulted in active bacterial activities. Overall, the spatial differences in water properties between the two regions had large influences on the regional distributions of riverine and marine DOC.

Plain Language Summary The Arctic Ocean is experiencing rapid environmental changes due to accelerated warming, a decline in sea ice coverage, and an increase in river discharge from Arctic rivers. However, it is not clear how these environmental changes affect the Arctic carbon cycle, particularly the quality and quantity of dissolved organic carbon (DOC). In this study, we used physical, chemical, and biological hydrographic datasets obtained from the western Arctic Ocean during the summer of 2018 and distinguished riverine and marine DOC from bulk DOC to clearly understand their distributions and utilization. The spatial distributions of riverine and marine DOC showed clear distinctions in their distributions between the Chukchi Borderland (CBL)/northern Chukchi Sea (NCS) and East Siberian Sea (ESS)/Mendeleyev Ridge (MR) regions. The high riverine DOC concentration in the CBL/NCS region was associated with the regional characteristics, including the accumulation of freshwater, strong stratification, and a longer residence time. On the other hand, anomalously high primary production was observed in the ESS/MR region, resulting in the large contribution of marine DOC. Our results highlight that the regional characteristics of water properties in the study region exerted significant influences on the spatial distributions of riverine and marine DOC.

Key Points:

- Riverine and marine dissolved organic carbon (DOC) were distinguished using hydrographic datasets obtained from the western Arctic Ocean
- Spatial distribution of riverine DOC showed higher abundance in the Chukchi Borderland and the northern Chukchi Sea
- Anomalously high primary production by the upwelling event enhanced marine DOC production in the East Siberian shelf/slope region

Supporting Information:

Supporting Information may be found in the online version of this article.

Correspondence to:

J. Jung,
jinyoungjung@kopri.re.kr

Citation:

Jung, J., Lee, Y., Cho, K.-H., Yang, E. J., & Kang, S.-H. (2022). Spatial distributions of riverine and marine dissolved organic carbon in the western Arctic Ocean: Results from the 2018 Korean expedition. *Journal of Geophysical Research: Oceans*, *127*, e2021JC017718. https://doi.org/10.1029/2021JC017718

Received 23 JUN 2021
Accepted 12 JUL 2022

Author Contributions:

Conceptualization: Jinyoung Jung
Funding acquisition: Eun Jin Yang, Sung-Ho Kang

1. Introduction

Dissolved organic carbon (DOC) has been recognized as an important component because of its essential role in carbon sequestration within the marine carbon cycle and microbial food loop (Zhang et al., 2018). In the marine environment, DOC originates from either marine or terrestrial sources, and the behavior and cycling of DOC are different depending on its origin and composition (Lønborg et al., 2020). For example, plankton activity, including direct release from phytoplankton and release during grazing and viral lysis, produces bioavailable marine DOC (Carlson & Hansell, 2015). Bioavailable marine DOC is remineralized by heterotrophic bacteria through the microbial loop and converted to inorganic carbon such as carbon dioxide (CO_2) (Amon, 2004; Buchan et al., 2014). The bacteria-mediated transformation of DOC is a significant source of carbon and energy in aquatic environments (Landa et al., 2014). Heterotrophic bacteria also produce refractory DOC (Lechtenfeld et al., 2015; Ogawa et al., 2001), which is the most persistent carbon pool, with the potential to be stored for millennia in the

Investigation: Jinyoung Jung, Youngju Lee, Kyoung-Ho Cho
Project Administration: Eun Jin Yang
Writing – original draft: Jinyoung Jung
Writing – review & editing: Jinyoung Jung, Youngju Lee, Kyoung-Ho Cho, Eun Jin Yang, Sung-Ho Kang

ocean's interior (Carlson & Hansell, 2015; Hansell et al., 2009; Jiao et al., 2010). On the other hand, terrestrial DOC, primarily derived from carbon-rich soils and vegetation, is mainly delivered to the ocean, especially coastal waters, by river runoff (referred hereafter as riverine DOC) (Lønborg et al., 2020; Raymond & Spencer, 2015). In general, riverine DOC is thought to be refractory in nature owing to its apparent conservative mixing behavior and low biodegradability (e.g., Dittmar & Kattner, 2003; Lobbes et al., 2000; Mann et al., 2012). However, previous observations and experiments provided evidence that the biodegradability of riverine DOC is associated with seasonality, differences in the riverine DOC composition, and regional hydrology (Holmes et al., 2008; Mann et al., 2012; Tanaka et al., 2016; Wickland et al., 2012). Thus, changes in DOC composition caused by marine environmental changes could have significant impacts on the marine carbon cycle and ecosystem.

The Arctic Ocean has experienced rapid environmental changes, including accelerated warming (Ballinger et al., 2020) and a strongly declining summer sea ice extent that coincides with an intense loss of multi-year sea ice (Cavalieri & Parkinson, 2012; Perovich et al., 2020). The response of the Arctic marine system to these changes has the potential to influence ocean productivity and DOC cycling. For example, the reduced sea-ice coverage can result in significant seasonal production of marine DOC via primary production (e.g., Mathis et al., 2007; McGuire et al., 2009; Shen et al., 2018) owing to a longer growing season, an expanded area of open water, and the nutrient supply by shelfbreak upwelling (Arrigo & van Dijken, 2011, 2015; Lewis et al., 2020; Tremblay et al., 2011). In addition, the thawing of permafrost due to Arctic warming can affect the river water discharge and elevate the amount of riverine DOC discharged into the Arctic Ocean (Abbott et al., 2014; Frey & McClelland, 2009; Le Fouest et al., 2018; Opsahl et al., 1999; Schuur et al., 2015). Furthermore, massive input of river water strengthens the influence of riverine DOC in the Arctic Ocean more than in the other oceans (e.g., Cooper et al., 2005; Dittmar & Kattner, 2003; Goncalves-Araujo et al., 2016; Guéguen et al., 2007; Holmes et al., 2012; Peterson et al., 2002) because the Arctic Ocean receives a disproportionately high amount (approximately 10%) of the total global river runoff from Arctic rivers (McClelland et al., 2012). These characteristics in the Arctic Ocean make the dynamics of DOC complex. Thus, it is clear that in-situ measurements are required for improved quantification of the overall magnitude of marine and riverine DOC under changing Arctic hydrographic conditions.

Although bulk DOC concentration provides quantitative information regarding DOC production (or input) and consumption (or loss), previous studies have shown that the seasonal production of bioavailable marine DOC via primary production as well as the influence of riverine DOC is not apparently reflected in bulk DOC distribution in the western Arctic Ocean (e.g., the Chukchi and Beaufort Seas) (e.g., Davis & Benner, 2005; DeFrancesco & Guéguen, 2021; Jung, Son, et al., 2021; Mathis et al., 2007; Shen et al., 2012). For example, Davis and Benner (2005) reported that concentrations of bulk DOC did not exhibit a significant seasonal change in surface water of the Canada Basin, but dissolved amino acids concentrations (indicators of bioavailable DOC) increased by 45% between spring and summer. Similarly, Shen et al. (2012) reported that bulk DOC concentrations in shelf and slope-basin surface waters were not significantly different between the Chukchi and Beaufort Seas despite the higher productivity in the Chukchi Sea. This is probably because the elevated production of marine DOC in summer is masked by the concurrently enhanced input of riverine DOC, making the changes in bulk DOC concentrations less discernible during productive seasons (Shen, Fichot, et al., 2016). Furthermore, DeFrancesco and Guéguen (2021) found no interannual variation in bulk DOC concentration in the polar mixed layer of the Canada Basin over an 11-year period (2007–2017), although the composition of dissolved organic matter (DOM) showed pronounced changes over time. The aforementioned previous studies suggest that the seasonal variations in marine or riverine DOC are reflected in the composition of DOC but less in bulk DOC concentrations. Thus, it is necessary to distinguish marine or riverine DOC from bulk DOC, and the fate of riverine DOC and the production and degradation of marine DOC need to be assessed separately to better understand and estimate their relative contributions.

However, quantifying marine and riverine DOC and assessing their impact on the marine carbon cycle are still a challenge in the highly dynamic nature of the river-influenced Arctic Ocean. Considerable efforts have been devoted to distinguishing the source of DOC in the Arctic Ocean using the C/N ratio (e.g., Lobbes et al., 2000; Wheeler et al., 1997), the stable isotopes of carbon (e.g., Amon & Meon, 2004; Opsahl et al., 1999; Raymond et al., 2007), biomarkers (e.g., lignin phenols and amino acids; Benner et al., 2005; Davis & Benner, 2005; Shen et al., 2018), and optical properties (e.g., Goncalves-Araujo et al., 2016; Guéguen et al., 2012; Jung, Son, et al., 2021; Shen, Benner, et al., 2016; Stedmon et al., 2011). Nevertheless, previous results are still not enough

to present a comprehensive picture of the spatial distributions of marine and riverine DOC in the Arctic Ocean. For example, the differences in the C/N ratios of riverine (30–60) and marine DOM (10–20) have been used as a tracer for the origin of DOM (Amon, 2004; Davis & Benner, 2005; Lobbes et al., 2000). However, the C/N ratio of marine DOM depends on biological activity in the water mass, thereby resulting in large variability in the C/N ratio of DOM, especially in marine-dominated waters, mainly due to variable dissolved organic nitrogen (DON) concentrations (Anderson & Amon, 2015). Moreover, the number of observations for DON is relatively low compared to DOC in the Arctic Ocean (Amon, 2004), making the C/N ratio less useful for quantitative computations (Anderson & Amon, 2015). The stable isotopes of carbon (ratio of ^{13}C–^{12}C, $\delta^{13}C$) also have been used to distinguish riverine from marine DOM in the Arctic because they show a distinction between riverine (−25‰ to −28‰, Opsahl et al., 1999; Amon & Meon, 2004; Raymond et al., 2007) and marine DOM (−21 ‰, Opsahl et al., 1999). Although the isotopic composition of DOC is a powerful tracer, it is also cumbersome to measure because of sample preparation (e.g., removing dissolved inorganic carbon (DIC) and oxidation of organic molecules into CO_2) and large volumes of seawater necessary. In addition, there is little observational data available for Arctic Ocean DOM $\delta^{13}C$ (Anderson & Amon, 2015; Beaupré, 2015 and references therein). For the biomarkers, lignin phenols are unequivocal tracers for riverine DOM due to their exclusively terrestrial origin and have been used to estimate the contribution of riverine DOC in the Arctic Ocean (Benner et al., 2005; Kattner et al., 1999; Lobbes et al., 2000; Opsahl et al., 1999). In comparison, amino acids have been used as qualitative indicators of the diagenetic state and bioavailability of organic matter (e.g., labile DOC, Davis & Benner, 2005) rather than marine source identification due to their preferential loss during degradation (Anderson & Amon, 2015). The optical properties of DOM, such as chromophoric dissolved organic matter (CDOM) and fluorescence dissolved organic matter (FDOM), have proven to be useful tracers for riverine (e.g., humic-like substances) and marine DOM (e.g., protein-like substances) as well (Coble, 1996, 2007; Stedmon et al., 2003). However, the optical properties of DOM are semi-quantitative without a combination of biomarker analyses (Anderson & Amon, 2015; Walker et al., 2013). In addition, few studies have examined the spatial distributions of both marine and riverine DOC simultaneously.

In this study, we attempted to distinguish marine and riverine DOC from bulk DOC by using stable oxygen isotope ratio ($\delta^{18}O$) and DOC concentrations in seawater and sea ice core samples collected from the western Arctic Ocean. This study simultaneously provides quantitative and qualitative estimates of marine and riverine DOC in the western Arctic Ocean. Therefore, the results for the spatial distributions and behaviors of marine and riverine DOC from this study would be valuable for filling the data gap, especially for the west region of the western Arctic Ocean.

2. Materials and Methods

2.1. Hydrographic Survey and Sampling

The 2018 Arctic expedition was conducted from 6 August to 24 August 2018 (the ARA09B cruise) on board the Korean icebreaker IBR/V *Araon* in the western Arctic Ocean (Figure 1). A total of 26 stations were occupied and geographically divided into two regions: the Chukchi Borderland (CBL)/northern Chukchi Sea (NCS) region (stations 1–7, 19–24, 26, and 27) and the East Siberian Sea (ESS)/Mendeleyev Ridge (MR) region (stations 8–18). The hydrographic characteristics of the water column were assessed from vertical profiles acquired from a conductivity-temperature-depth (CTD) (SeaBird Electronics, SBE 911 plus) profiler. Seawater samples were collected using Niskin bottles at surface and discrete depths chosen based on CTD profiles. The mixed layer depth (MLD) was estimated from the CTD profile and is defined as the depth at which the density change exceeded 0.05 kg m^{-3} relative to the reference value at a 5 m depth (Lee et al., 2019; Venables & Moore, 2010). Further details on the hydrographic survey stations, including locations, water depths, and MLDs, are given in Table S1 in Supporting Information S1.

Seawater samples for DOC and $\delta^{18}O$ were gravity filtered through pre-combusted (at 550°C for 6 hr) Whatman GF/F filters (Chen et al., 2018; Jung, Son, et al., 2021). For DOC measurement, the filtrate was stored frozen (−24°C) in two pre-combusted 20 ml glass ampoules until analysis. For $\delta^{18}O$ measurement, the filtrate was distributed into an acid-cleaned 20 ml glass vial, which was sealed with parafilm and stored at 4°C until analysis. For nutrient measurement, seawater was drawn from the Niskin bottles into 50 ml conical tubes and immediately stored in a refrigerator at 4°C prior to chemical analysis. Seawater samples for chlorophyll-a (Chl-a) and heterotrophic bacterial abundance measurements were collected in the upper 150 m and then processed for analyses.

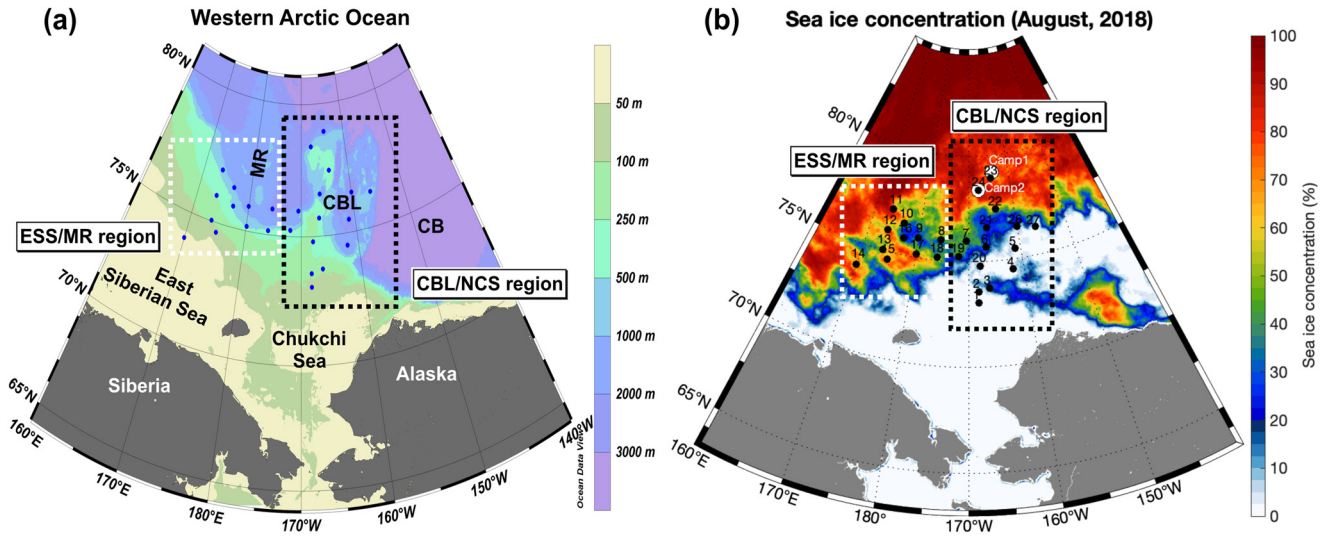

Figure 1. Maps showing (a) bathymetric features of the study area and locations of the hydrographical survey stations (blue circles) and (b) mean sea ice concentration for August 2018. In (b), the locations and the numbers of the sampling stations (black circles) and sea ice camps (white circles) are superimposed onto the mean sea ice concentrations derived from Advanced Microwave Scanning Radiometer two sea ice concentration data for August 2018. Geographical locations are abbreviated as follows: Canada Basin, Chukchi Borderland (CBL), and Mendeleyev Ridge (MR). Geographic locations are divided into two regions: the CBL/northern Chukchi Sea region (stations 1–7, 19–24, 26, and 27 enclosed by black dashed lines) and the East Siberian Sea/MR region (stations 8–18 enclosed by white dashed lines). Figure 1(a) was illustrated using Ocean Data View software (Schlitzer, 2021).

During the cruise, a total of four ice core samples were collected from two sea ice camp stations (camp 1: N79°12.1564′, W164°9.119′ and camp 2: N78° 24.3459′, W167°47.7426′) in the CBL, using a 9.5 cm diameter ice corer (fiberglass core barrel with stainless steel cutters powered by a portable generator and electric drill) (Figure 1). The ice cores were cut into 10 cm long pieces with a commercial band saw that was carefully cleaned with Milli-Q water before every cut. The subsamples were placed in clean plastic bags (polyethylene) and transported to the laboratory on board the vessel for further processing. The ice core samples were thawed in the dark at 4°C. Before filtration, the samples were homogeneously mixed, transferred into acid-cleaned 4 L-carboys, and then gravity-filtered using the same method for seawater DOC sampling.

2.2. Dissolved Organic Carbon Measurement

DOC concentrations were measured by high temperature combustion (680°C) using a Shimadzu TOC-L analyzer. A standard curve was established with potassium hydrogen phthalate before sample analysis. Deep-sea reference seawater (42–45 μM C for DOC) from the University of Miami consensus reference material program was used as a quality control standard for DOC samples. Based on repeated measurements (at least three measurements per sample), analytical errors were within 5% (Chen et al., 2018; Jung, Son, et al., 2021).

2.3. Stable Oxygen Isotope Ratios Measurement

$\delta^{18}O$ was measured with a stable isotope ratio mass spectrometer (Isoprime, Micromass, Manchester, UK) connected to a CO_2–H_2O equilibration unit at the Korea Basic Science Institute. $\delta^{18}O$ was determined with respect to the Vienna-Standard Mean Ocean Water (V-SMOW) standard. The $\delta^{18}O$ was obtained as follows:

$$\delta^{18}O = \left[\left({}^{18}O/{}^{16}O_{sample}/{}^{18}O/{}^{16}O_{V\text{-}SMOW}\right) - 1\right] \times 1000 \quad (1)$$

The precision based on repeated measurements of an internal standard was determined to be <0.1‰.

2.4. Nutrient Measurement

Nutrients, including nitrite + nitrate ($NO_2 + NO_3$), phosphate (PO_4), ammonium (NH_4), and silicic acid ($Si(OH)_4$), were measured onboard using a four-channel Auto-Analyzer (QuAAtro, Seal Analytical, Germany), according to

Table 1
End-Member Values Used in Mass Balance Calculations

End-member	Salinity (psu)	$\delta^{18}O$ (‰)
River water (f_{river})	0	−20 ± 1.0
Sea-ice meltwater ($f_{sea\ ice\ melt}$)	4 ± 1.0	−2 ± 1.0
Seawater ($f_{seawater}$)	34.8 ± 0.1	0.28 ± 0.03

Note. For further explanation, see the text in Section 2.7.1.

the Joint Global Ocean Flux Study (JGOFS) protocols described by Gordon et al. (1993). Nutrient reference materials for seawater provided by KANSO Techno (Lot. No. BV) were measured along with standards for every batch of runs to assess the accuracy and reproducibility. The precision for $NO_2 + NO_3$, PO_4, and $Si(OH)_4$ was ±0.14, ±0.02, and ±0.28 μmol kg^{-1}, respectively.

2.5. Chlorophyll-a Measurement

Seawater samples for Chl-a measurements were filtered through 47 mm GF/F filters, then extracted with 90% acetone for 24 hr. Chl-a was measured using a fluorometer (Trilogy, Turner Designs, USA) (Lee et al., 2019).

2.6. Heterotrophic Bacterial Abundance

Seawater samples for the determination of heterotrophic bacterial abundance were fixed for 15 min in 1% (v/v) paraformaldehyde (final concentration) and stored at −80°C prior to analysis. To enumerate heterotrophic bacteria, the samples were thawed, stained with 1:10,000 (v:v) SYBR Green I (Molecular Probes) for 15 min, and then analyzed using an Accuri C6 flow cytometer (Becton Dickinson, USA) equipped with an air-cooled argon laser (488 nm, 15 mW) within 1 month of the cruise (Marie et al., 1997; Pan et al., 2005). Bacteria were identified based on their side light scatter and green fluorescence signals. All the cytometric data analyses were performed using FlowJo software (Tree Star, USA).

2.7. Calculation

2.7.1. Freshwater Components

The fractions of river water (f_{rw}), sea-ice meltwater (f_{sim}), and seawater (f_{sw}) were estimated using mass balance calculations as was previously done in the Arctic Ocean (e.g., Guéguen et al., 2007; Mathis et al., 2007; Yamamoto-Kawai et al., 2008). We used a three-endmember mass balance approach, employing salinity and $\delta^{18}O$ as tracers. This approach assumes that the observed salinity and $\delta^{18}O$ values in the water samples have resulted from a mixture of river water, sea ice meltwater, and seawater. These respective fractions were calculated using the following mass balance equations:

$$f_{rw} + f_{sim} + f_{sw} = 1 \quad (2)$$

$$f_{rw} \times \delta^{18}O_{rw} + f_{sim} \times \delta^{18}O_{sim} + f_{sw} \times \delta^{18}O_{sw} = \delta^{18}O_{ob} \quad (3)$$

$$f_{rw} \times S_{rw} + f_{sim} \times S_{sim} + f_{sw} \times S_{sw} = S_{ob} \quad (4)$$

where f and S refer to the fraction and salinity, respectively. $\delta^{18}O_{ob}$ and S_{ob} are the observed values for each seawater sample. The three end-member values of $\delta^{18}O$ and S used for the calculation are summarized in Table 1, together with the observed data from previous studies. The details behind the choice of end-member values can be found in Jung, Son, et al. (2021) and other references (e.g., Bauch, 1995; Ekwurzel et al., 2001; Eicken et al., 2002; Pfirman et al., 2004; Mathis et al., 2007; Cooper et al., 2008; Yamamoto-Kawai et al., 2008; Logvinova et al., 2016). In brief, the S of river water, sea ice meltwater, and seawater were 0, 4, 34.8 psu, respectively, and the $\delta^{18}O$ end-members −20‰, −2‰, and 0.28‰, respectively. The uncertainties of f_{rw}, f_{sim}, and f_{sw}, owing to uncertainties in the range of end-member S and $\delta^{18}O$ data (Table 1), remain an average within ±0.01.

2.7.2. Riverine Dissolved Organic Carbon

Riverine DOC concentration (μM C) was determined using the following equation as described in Mathis et al. (2007):

$$\text{Riverine DOC} = f_{rw} \times DOC_{rw} \quad (5)$$

where DOC_{rw} refers to the initial DOC concentration in river runoff. Mathis et al. (2007) used a concentration of 350 μM C for initial DOC concentrations in river runoff in the Chukchi Sea (i.e., historic observation value from the Yukon River). However, river runoff in the western Arctic Ocean can be derived from the North

American and East Siberian rivers and the Bering Strait inflow (e.g., Cooper et al., 2005; Morison et al., 2012; Yamamoto-Kawai et al., 2005, 2009). Thus, as described in detail in Jung, Son, et al. (2021), it is not reasonable to use the average DOC concentration in the major Arctic rivers draining into the western Arctic owing to the degradation of riverine DOC during its transport from the Arctic rivers (Alling et al., 2010; Cooper et al., 2005; Hansell et al., 2004; Letscher et al., 2011). In this study, we used the zero-salinity (100% river water) DOC value obtained from the relationship between DOC and S as a DOC_{rw}. However, the DOC concentration and S can be diluted by sea ice meltwater in the western Arctic Ocean during the summer season (Mathis et al., 2005). Thus, sea ice meltwater-corrected S ($S_{sim\text{-}corrected}$) calculated by the following equation needs to be used to correct the effects of sea ice meltwater on DOC concentration and S (Yamamoto-Kawai et al., 2009):

$$S_{sim\text{-}corrected} = (S - S_{sim} f_{sim}) / (1 - f_{sim}) \quad (6)$$

where the calculated $S_{sim\text{-}corrected}$ indicates S in waters that are not influenced by sea ice meltwater. During the cruise, a statistically significant inverse relationship was found between DOC concentration and $S_{sim\text{-}corrected}$ ($DOC = -3.07 \times S_{sim\text{-}corrected} + 163$, $r^2 = 0.55$, $p < 0.01$) (Figure S1 in Supporting Information S1). The zero-salinity intercept of 163 μM C for DOC was similar to those obtained for the western Arctic ($DOC = -3.85 \times S_{sim\text{-}corrected} + 190$, Jung, Son, et al., 2021), the northeastern Chukchi Sea ($DOC = -3.63 \times S + 186$, Mathis et al., 2009), and the Beaufort Gyre ($DOC = -2.60 \times$ salinity $+ 154$, Hansell et al., 2004). Therefore, a value of 163 ± 5.5 μM C (95% confidence level) was taken as representative of the riverine DOC concentration that entered the study region (i.e., DOC_{rw}). The uncertainty of riverine DOC, due to uncertainties in the range of DOC_{rw} (i.e., 163 ± 5.5 μM C), was estimated to be ±0.63 μM C.

2.7.3. Marine Dissolved Organic Carbon

Marine DOC concentration (μM C) was estimated using the following equation reported by Mathis et al. (2007):

$$\text{Marine DOC} = \text{Measured DOC} - (f_{rw} \times DOC_{rw} + f_{sim} \times DOC_{sim}) \quad (7)$$

where DOC_{sim} refers to the DOC concentration in the sea ice (μM C). As shown in Figure S2 in Supporting Information S1, the DOC_{sim} values obtained from four sea ice core samples ranged from 10.8 to 27. 4 μM C, with an average of 17 ± 4.5 μM C. The mean DOC_{sim} obtained from this study was similar to that (21.5 μmol kg^{-1}) observed previously in the ice cores collected from the Chukchi shelf in the spring of 2002 (Mathis et al., 2007). However, the DOC_{sim} values were substantially lower than the DOC concentrations in the surface layer (see Section 3.3). Amon (2004) reported that DOC is rejected from sea ice during its formation. Thus, lower DOC_{sim} values are commonly observed due to the release of DOC by rejected brine from sea ice during winter (Giannelli et al., 2001). In this study, we used the mean DOC_{sim} value (i.e., 17 ± 4.5 μM C) for the calculation of marine DOC, although the variability of DOC_{sim} is most likely related to where the ice forms and the biogeochemical properties of the water below the ice (Mathis et al., 2007; Thomas et al., 2001). The uncertainty of marine DOC was estimated to be ±0.64 μM C by calculating the propagating errors of each parameter.

3. Results

3.1. Surface Distributions of Freshwater Components

Surface distributions of sea surface salinity (SSS), temperature (SST), f_{rw}, and f_{sim} in the western Arctic Ocean showed an east–west gradient (Figure 2). Relatively warmer (−0.82 ± 0.45°C) and fresher waters (28 ± 0.69 psu) were observed in the CBL/NCS region (i.e., stations 1–7, 19–24, 26, and 27). In contrast, the ESS/MR region (i.e., stations 8–18) was characterized by colder (−1.3 ± 0.23°C) and saline waters (30 ± 0.73 psu) (Figures 2a and 2b). The f_{rw} values in the CBL/NCS region (0.17 ± 0.026) were higher than those in the ESS/MR region (0.11 ± 0.034), exhibiting a clear distinction in surface distribution between the CBL/NCS and ESS/MR regions (Figure 2c). The f_{sim} values in the CBL/NCS region (0.037 ± 0.018) were also slightly higher than those in the ESS/MR region (0.032 ± 0.017) (Figure 2d). The higher f_{rw} and f_{sim} values in the CBL/NCS region coincided with the low SSS and relatively high SST (Figures 2a and 2b) as well as an absence of sea ice (Figure 1). These results imply that both river water and sea ice meltwater contributed largely to the surface freshening in the CBL/NCS region.

The plot of $\delta^{18}O$ versus S shows that the western Arctic waters in the summer of 2018 did not deviate significantly from a mixing line between the seawater end-member and river runoff (Figure 3). Instead, they were affected by a

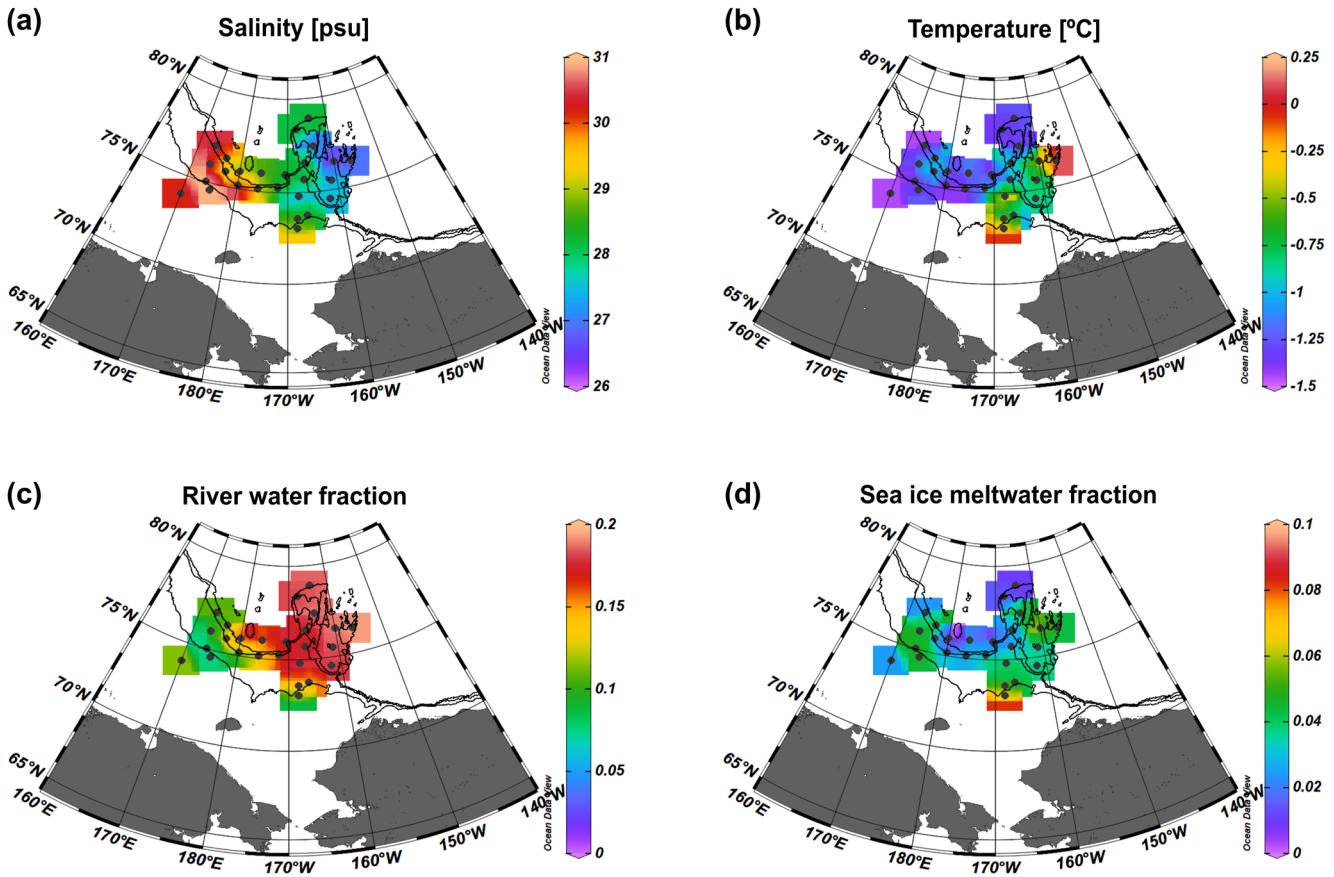

Figure 2. Surface distributions of (a) sea surface salinity (SSS), (b) sea surface temperature, (c) river water (f_{rw}), and (d) sea ice meltwater (f_{sim}) fractions in the western Arctic Ocean during the summer of 2018. All surface samples were collected at a depth of 3 m. The black contours indicate isobaths of 100, 500, 1,000 m. Figures were illustrated using Ocean Data View software (Schlitzer, 2021).

seasonally varying signal from ice that pulled toward the right in winter (sea-ice formation) and toward the left in summer (sea-ice melt) (Cooper et al., 2016; Macdonald et al., 2002). The large river runoff signal indicates that the influence of river runoff overwhelmed that of sea ice meltwater and that river runoff is the major source of freshwater in the western Arctic (Jung, Son, et al., 2021). However, $\delta^{18}O$ and S in the western Arctic vary seasonally and spatially (Cooper et al., 2016; Yamamoto-Kawai et al., 2008). Pronounced seasonal variations in freshwater flowing through the Bering Strait (Woodgate & Aagaard, 2005), river runoff fluxes (Holmes et al., 2012), and seasonal sea ice retreat (Årthun et al., 2021; Comiso et al., 2017) are known as the causes of the variation. Thus, the spatial distribution of freshwater components from this study should be considered as a summertime snapshot of freshwater distribution in 2018.

3.2. Spatial Distributions of Nutrients and Chl-a

3.2.1. Surface Distribution

During the cruise, surface concentrations of $NO_2 + NO_3$ and PO_4 ranged from below the detection limit to 3.0 and 0.48–1.2 μmol kg^{-1}, with averages of 0.16 ± 0.6 and 0.62 ± 0.16 μmol kg^{-1}, respectively (Figures 4a and 4b). The $NO_2 + NO_3$ and PO_4 concentrations were lowest in the CBL/NCS region, whereas the highest $NO_2 + NO_3$ and PO_4 concentrations were observed in the ESS/MR region, especially in the East Siberian shelf/slope region. The highest nutrient concentrations coincided with the highest SSS in the ESS/MR region (Figure 2a).

Similarly, surface Chl-a concentration showed a regional difference between the two regions (Figure 4c). In the CBL/NCS region, the surface Chl-a concentrations were extremely low (0.02–0.12 mg m^{-3}) due to low

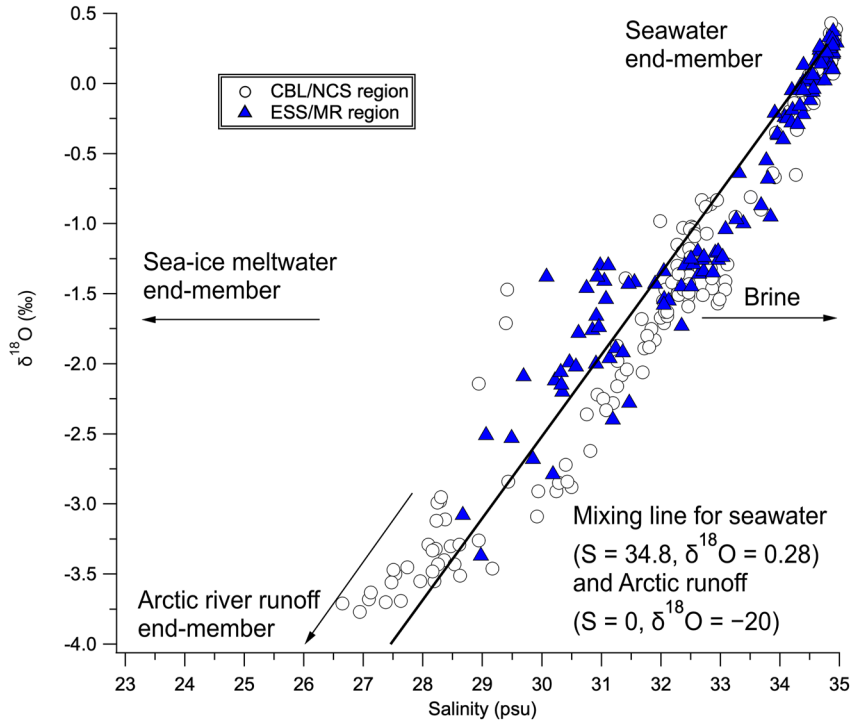

Figure 3. Relationship between $\delta^{18}O$ (‰) and salinity (S) (psu) in seawater samples collected in the Chukchi Borderland/northern Chukchi Sea (white circles) and East Siberian Sea/Mendeleyev Ridge (blue triangles) regions during the summer of 2018. Arrows indicate mixing with river runoff, sea-ice meltwater, and brine. Black line is the expected mixing line between seawater ($S = 34.8$ psu, $\delta^{18}O = 0.28$‰) and Arctic river runoff ($S = 0$ psu, $\delta^{18}O = -20$‰).

$NO_2 + NO_3$ concentrations. On the other hand, the highest Chl-a concentrations (0.03–9.5 mg m^{-3}) were observed in the ESS/MR region, which was associated with the highest surface nutrients and SSS.

3.2.2. Vertical Distribution

Mean vertical profiles of $NO_2 + NO_3$, PO_4, and Chl-a concentrations are presented in Figure 5. In the CBL/NCS region, the $NO_2 + NO_3$ concentration was depleted in the upper 25 m (Figure 5a). However, it sharply increased with depth, reaching a maximum value of 16 ± 7.5 μmol kg^{-1} at 55 m, and then gradually decreased with depth to relatively constant values of 12 ± 0.74 μmol kg^{-1} at depths of 200–500 m. The PO_4 concentration varied from 0.53 to 1.9 μmol kg^{-1}, showing a similar distribution pattern to $NO_2 + NO_3$ (Figure 5b). The Chl-a concentration was quite low in the upper 25 m (0.13 ± 0.12 mg m^{-3}) but increased with depth, showing a subsurface Chl-a maximum (SCM) (2.2 mg m^{-3}) at depths of 45–50 m (Figure 5c).

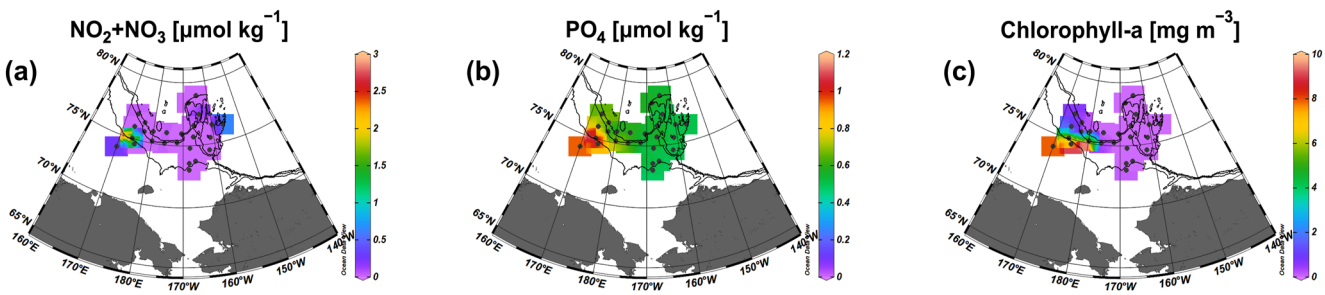

Figure 4. Surface distributions of (a) nitrite + nitrate ($NO_2 + NO_3$) (μmol kg^{-1}), (b) phosphate (PO_4) concentrations (μmol kg^{-1}), and (c) chlorophyll-a (mg m^{-3}) in the western Arctic during the summer of 2018. All surface samples were collected at a depth of 3 m. The black contours indicate isobaths of 100, 500, 1,000 m. Figures were illustrated using Ocean Data View software (Schlitzer, 2021).

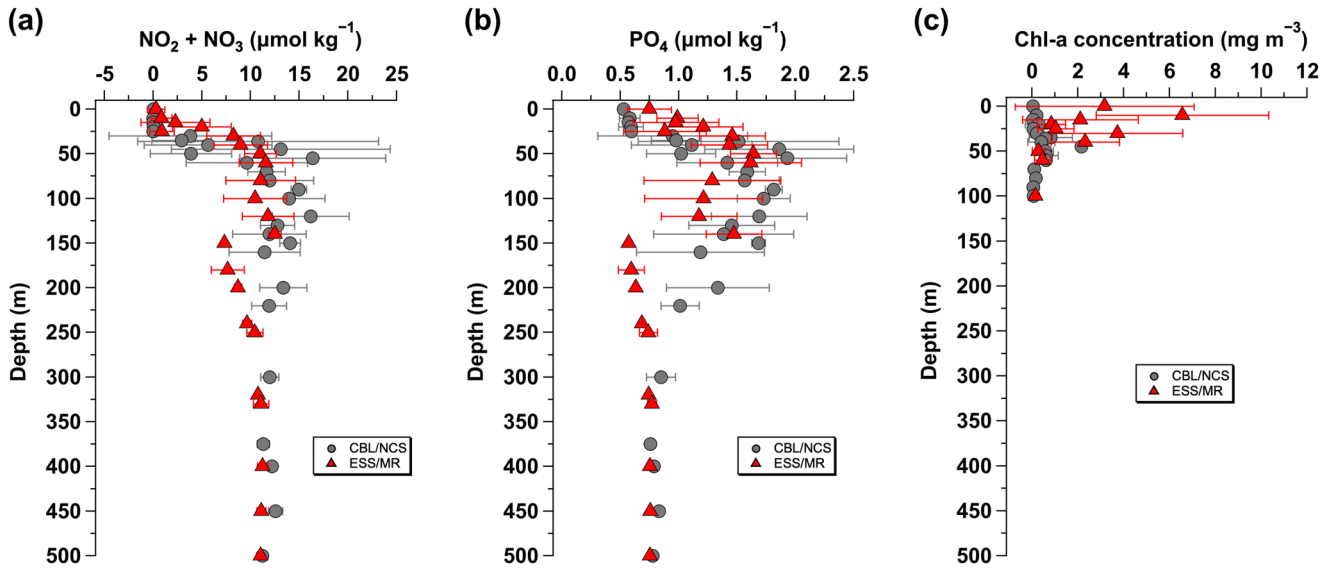

Figure 5. Mean vertical profiles of (a) nitrite + nitrate ($NO_2 + NO_3$) (μmol kg^{-1}), (b) phosphate (PO_4) (μmol kg^{-1}), and chlorophyll-a (mg m^{-3}) concentrations observed in the Chukchi Borderland/northern Chukchi Sea (solid gray circles) and East Siberian Sea/Mendeleyev Ridge (solid red triangles) regions in the summer of 2018. Error bars represent standard deviations.

The vertical distributions of $NO_2 + NO_3$ and PO_4 concentrations observed in the ESS/MR region were similar to those in the CBL/NCS region. However, remarkable differences in the vertical distributions between the two regions were the $NO_2 + NO_3$ and PO_4 concentrations in the upper 25 m. Compared to those in the CBL/NCS region, the $NO_2 + NO_3$ and PO_4 concentrations in the upper 25 m of the ESS/MR region were higher (1.9 ± 1.9 μmol kg^{-1} for $NO_2 + NO_3$ and 0.96 ± 0.17 μmol kg^{-1} for PO_4). As a result, the Chl-a concentrations observed in the upper 25 m of the ESS/MR region were relatively higher than those observed in the SCM layer of the CBL/NCS region.

Figure 6 shows a detailed water column structure across the East Siberian and Chukchi shelf and slope regions. The vertical sections of S and potential temperature (θ) in the Chukchi shelf and slope region (stations 4, 18–20) show the presence of surface mixed layer (<25 m depth) and Pacific summer water ($S = 31$–32 psu, θ maximum) at depths of 30–60 m (Codispoti et al., 2005; Nishino et al., 2013). In addition, the intense stratification caused by freshwater input ($S < 28$ psu) (Figure 6b) restricted the nutrient supply from deep layers (Figures 6d and 6e), resulting in the development of the SCM at the upper end of the nitracline (depths of 30–50 m) (Figure 6f).

In contrast, the Pacific summer water was not found in the East Siberian shelf and slope region (stations 14, 15, and 17). Instead, temperature minimum water at $S \approx 32$ was observed at depths between 30 and 40 m. In addition, an outstanding feature of the nutrient-rich Pacific winter water ($S \approx 33$ psu, θ minimum, Nishino et al., 2013) was observed at depths between 40 and 80 m (Figures 6b–6e). Furthermore, the extremely high Chl-a concentrations in the upper 20 m (8.4 ± 0.91 mg m^{-3}) were accompanied by relatively higher S and the shoaling of the nutricline.

3.3. Surface Distributions of Riverine and Marine DOC

Surface bulk DOC concentrations ranged from 65 to 83 μM C, with an average of 71 ± 4.4 μM C (Figure 7a), which is similar to values previously observed in the western Arctic during summer (Jung, Son, et al., 2021; Letscher et al., 2011; Shen et al., 2018; Tanaka et al., 2016). The surface bulk DOC concentration showed no clear distinction in distribution between the CBL/NCS (range: 65–76 μM C and mean: 70 ± 3.2 μM C) and ESS/MR regions (range: 66–83 μM C and mean: 74 ± 5.0 μM C), unlike other variables such as SSS and f_{rw}. However, the surface distributions of the estimated riverine and marine DOC exhibited clear distinctions in their distributions between the two regions.

The surface distribution of the estimated riverine DOC and its contribution to the observed bulk DOC are shown in Figures 7b and 7c, respectively. In the CBL/NCS region, riverine DOC concentrations ranged from 14 to

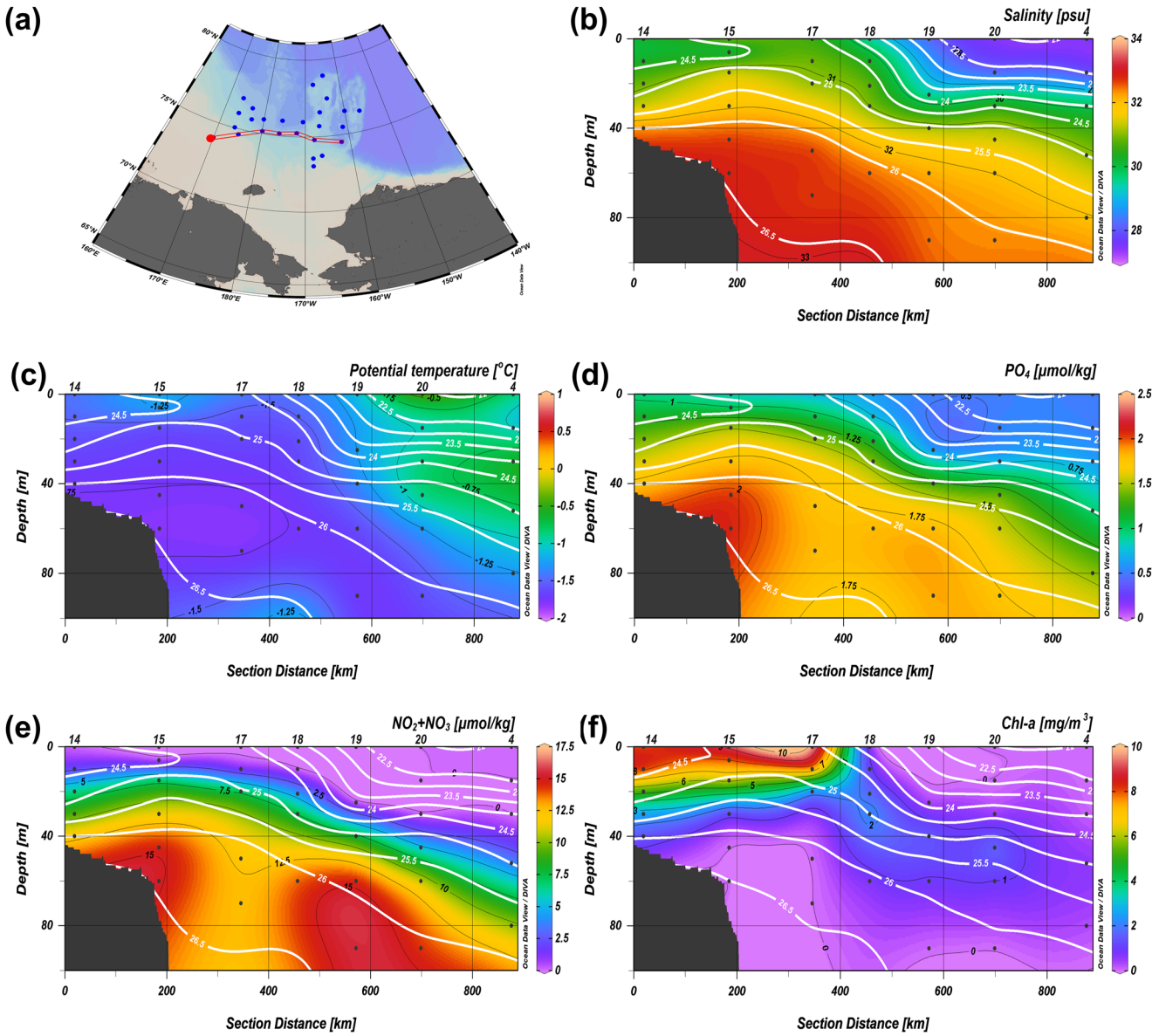

Figure 6. Vertical sections across the East Siberian and Chukchi shelf and slope regions in the summer of 2018. (a) Map of stations occupied during the cruise. The stations enclosed by the red rectangle were used to illustrate the vertical sections. Vertical sections of (b) salinity (S) (psu), (c) potential temperature (θ) (°C), (d) phosphate (PO_4) (µmol kg^{-1}), (e) nitrite + nitrate ($NO_2 + NO_3$) (µmol kg^{-1}), and chlorophyll-a (mg m^{-3}). Black lines and black numbers show the contours and values of each variable. Density (kg m^{-3}) contours (white thick lines and white numbers) are superimposed on the panels of (b–f). Station numbers are shown at the top of each figure. Figures were illustrated using Ocean Data View software (Schlitzer, 2021).

31 µM C, with an average of 28 ± 4.2 µM C. The mean contribution of riverine DOC was 40 ± 5.7% (range: 22–47%) of the observed bulk DOC. In comparison, the riverine DOC concentrations in the ESS/MR region ranged from 12 to 29 µM C, with an average of 19 ± 5.6 µM C, which accounted for 26 ± 8.5% (range: 15–44%) of the observed bulk DOC.

On the other hand, the estimated marine DOC showed the opposite variation trend, with the lower values occurring in the CBL/NCS region (mean: 41 ± 3.9 µM C and range: 33–50 µM C) and higher values occurring in the ESS/MR region ranging from 38 to 64 µM C (mean: 54 ± 8.1 µM C) (Figure 7d). The contributions of marine DOC to the observed bulk DOC in the CBL/NCS and ESS/MR regions were found to represent 51–76% (mean: 59 ± 5.4%) and 56–83% (mean: 73 ± 8.2%), respectively (Figure 7e). Although most of the observed DOC was estimated to be marine DOC, heterotrophic bacterial abundance values were remarkably low in the CBL/NCS

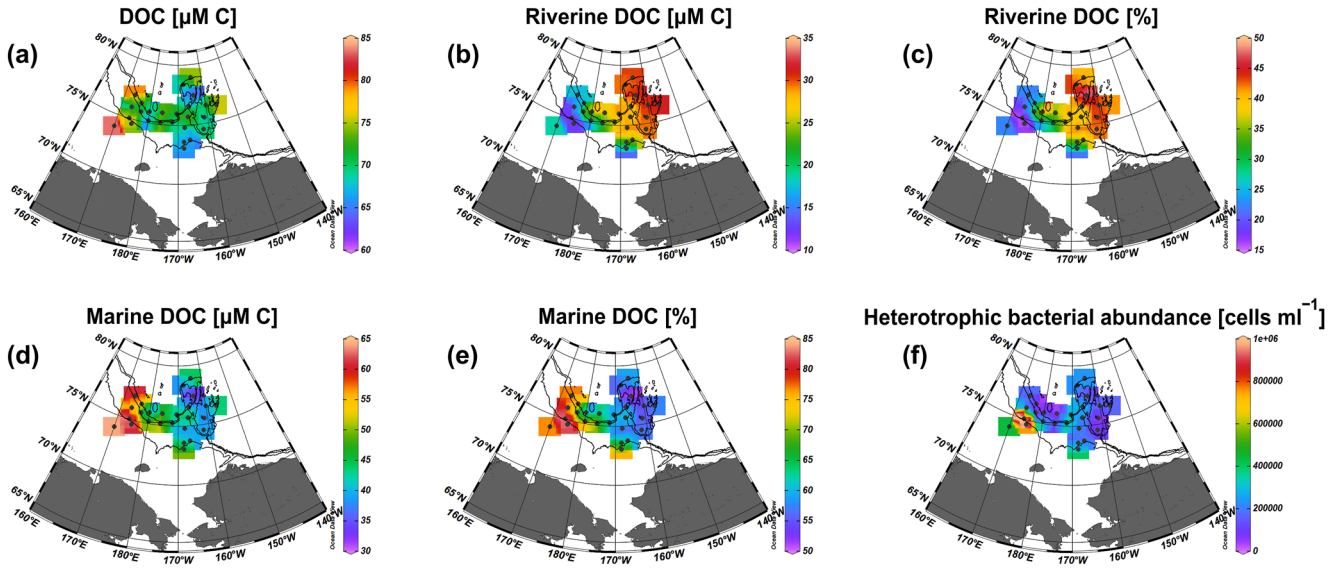

Figure 7. Surface distributions of (a) dissolved organic carbon (DOC) concentration (μM C), (b) riverine DOC concentration (μM C), (c) contribution of riverine DOC to the observed DOC (%), (d) marine DOC concentration (μM C), (e) contribution of marine DOC to the observed DOC (%), and (f) heterotrophic bacterial abundance (cells ml^{-1}) in the western Arctic during the summer of 2018. All surface samples were collected at a depth of 3 m. The black contours indicate isobaths of 100, 500, 1,000 m. Figures were illustrated using Ocean Data View software (Schlitzer, 2021).

region, where the contributions of riverine DOC were relatively high (Figure 7f). In addition, the prevalence of marine DOC in the ESS/MR region was consistent with high heterotrophic bacterial abundance, which was associated with extremely high surface Chl-a concentrations (Figure 4c) sustained by nutrient supply (Figures 4a and 4b) during the sampling periods. These results suggest that the active production of marine DOC by marine biological activities sustained high heterotrophic bacterial abundances in the ESS/MR region.

3.4. Vertical Distributions of Riverine and Marine DOC

The vertical distributions of bulk DOC, riverine and marine DOC, and their contributions to the bulk DOC at all stations are shown in Figure 8. The vertical distributions of bulk DOC concentrations generally showed a pattern of decreasing concentration from the surface to the bottom layers (Figure 8a). The bulk DOC concentrations were low and relatively constant (52 ± 5.2 μM C) at depths of 250–500 m, suggesting a broadly uniform background concentration of refractory DOC. No significant differences in bulk DOC concentrations were observed between the CBL/NCS (range: 40–84 μM C and mean: 63 ± 7.9 μM C) and ESS/MR regions (range: 40–85 μM C and mean: 65 ± 9.0 μM C). However, regional differences in riverine and marine DOC concentrations were found between the two regions.

The riverine DOC concentrations in the CBL/NCS region ranged from 0.15 to 31 μM C (mean: 15 ± 9.7 μM C), with the highest concentrations occurring in the surface waters and the lowest values occurring in the deep layers (Figure 8b). The contribution of riverine DOC in the CBL/NCS region varied from 0.28% to 47%, with an average of 22 ± 13% (Figure 8c). Meanwhile, the riverine DOC concentrations in the ESS/MR region exhibited a similar depth distribution, with an average of 9.9 ± 7.2 μM C (range: 0.11–29 μM C), which accounted for 14 ± 9.9% (range: 0.12–44%) of the bulk DOC. The vertical profile of riverine DOC clearly showed a pronounced accumulation of riverine DOC within the Beaufort Gyre (i.e., the CBL/NCS region).

It is worth mentioning that the MLD could influence the vertical distribution of riverine DOC. During the cruise, the MLD ranged from 6 to 16 m (mean: 9.3 ± 3.2 m), with slightly deeper depths in the CBL/NCS region (11 ± 3.0 m) and shallower ones in the ESS/MR region (7.5 ± 2.6 m) (Table S1 in Supporting Information S1). The shallower MLD in summer than in winter (Ulfsbo et al., 2014) suggests that most of the riverine DOC would be confined within the MLD. However, substantially higher riverine DOC and f_{rw} values compared to those in the deep layers (>250 m) were found in the upper halocline layer (32 psu < S < 33.5 psu at depths between 50 and 200 m, Codispoti et al., 2005; Alkire et al., 2019) (Figures 8b–8d), where f_{sim} dropped below zero (Figure 8e).

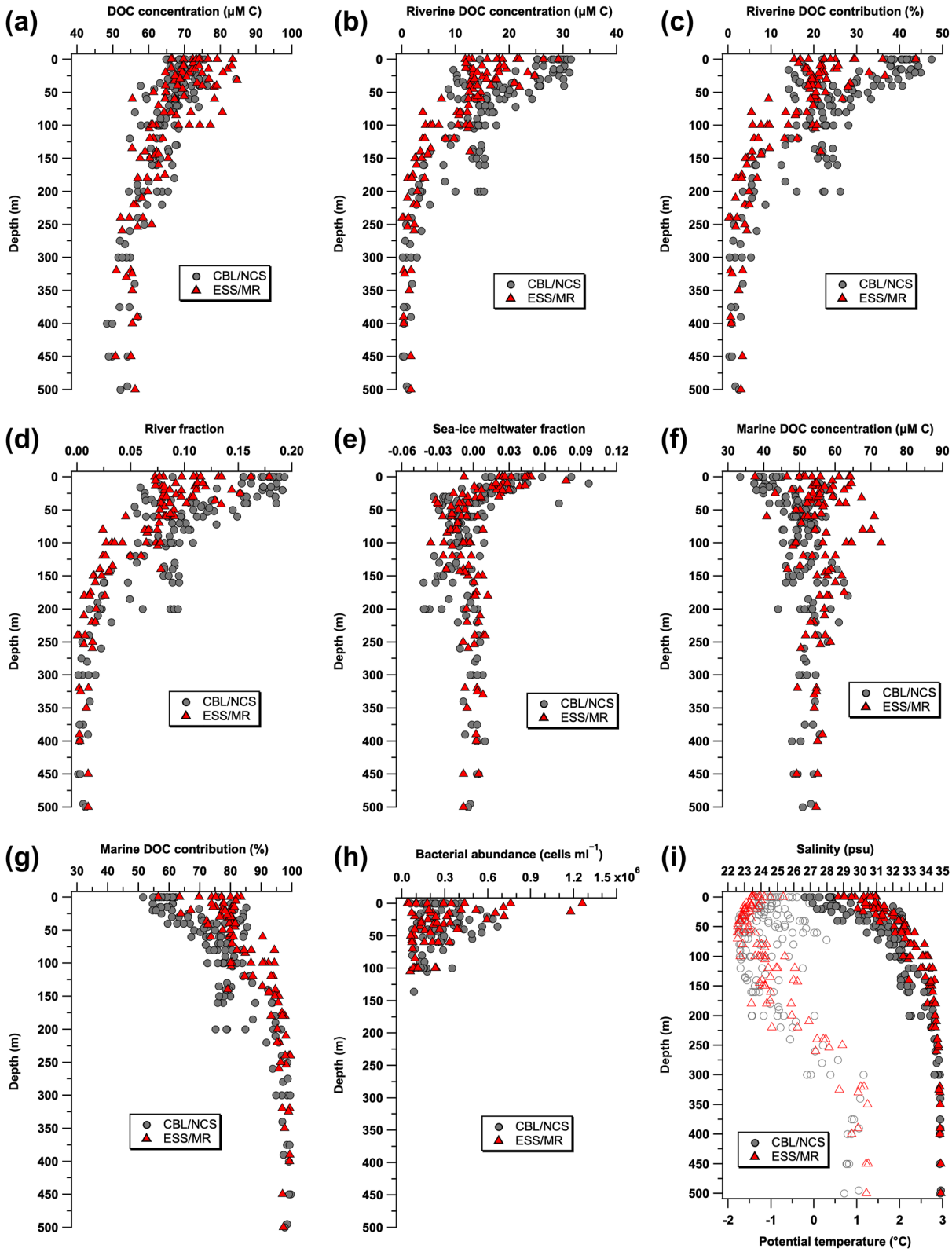

Figure 8. Vertical profiles of (a) dissolved organic carbon (DOC) (μM C), (b) riverine DOC (μM C), (c) riverine DOC contribution (%), (d) river fraction (f_{rw}), (e) sea-ice meltwater fraction (f_{sim}), (f) marine DOC (μM C), (g) marine DOC contribution (%), (h) bacterial abundance (cells ml^{-1}), and (i) salinity (S) (psu) and potential temperature (θ) (°C) observed in the Chukchi Borderland/northern Chukchi Sea (solid gray circles) and East Siberian Sea/Mendeleyev Ridge (solid red triangles) regions in the summer of 2018. Note that the vertical profiles of potential temperature observed in the two regions are shown as open symbols in (i).

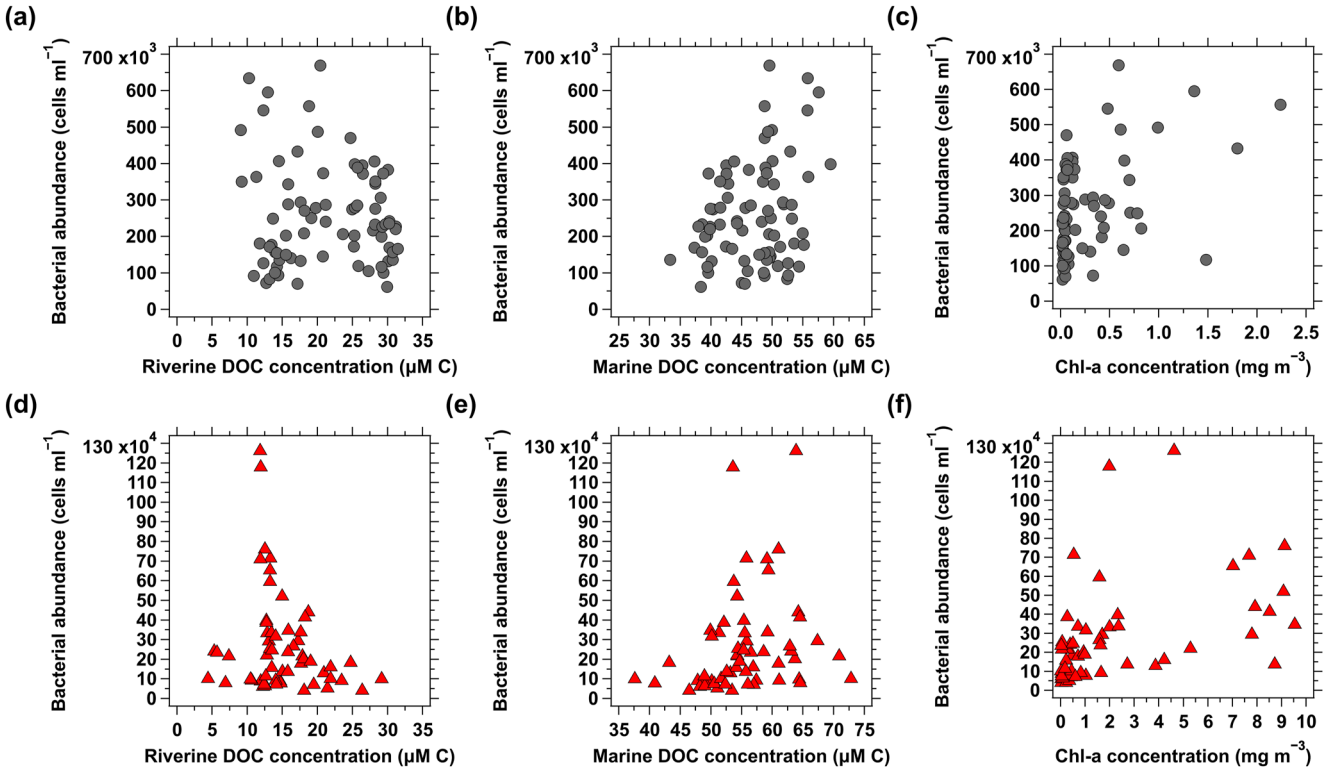

Figure 9. Scatterplots between bacterial abundance (cells ml^{-1}) and (a, d) riverine dissolved organic carbon (DOC) (μM C), (b, e) marine DOC (μM C), and (c, f) chlorophyll-a concentrations (mg m^{-3}) for the data set in the upper 100 m in the Chukchi Borderland/northern Chukchi Sea (solid gray circles) and East Siberian Sea/Mendeleyev Ridge (solid red triangles) regions.

Although marine DOC was the dominant DOC component in the CBL/NCS and ESS/MR regions, it showed apparent regional differences between the two regions (Figure 8f). In the CBL/NCS region, the marine DOC concentration ranged from 33 to 63 μM C (mean: 49 ± 5.5 μM C), with lower values in the surface waters. In comparison, the marine DOC in the ESS/MR region ranged from 38 to 73 μM C (mean: 55 ± 6.0 μM C) and exhibited a large degree of variability, with higher values in the upper 100 m. The contributions of marine DOC in the upper 100 m of the CBL/NCS and ESS/MR regions varied from 51% to 84% and 56%–94%, with averages of 69 ± 9.5% and 79 ± 6.7%, respectively (Figure 8g). In addition, heterotrophic bacterial abundance values were higher in the upper 50 m of the ESS/MR region than those of the CBL/NCS region (Figure 8h).

3.5. Relationships Between Heterotrophic Bacterial Abundance and Riverine or Marine DOC in the Western Arctic in the Summer of 2018

To explore the heterotrophic bacterial activity in response to riverine and marine DOC in the study region, we utilized the data set obtained in the upper 100 m because most heterotrophic bacterial abundances and Chl-a concentrations were measured solely in the upper 100 m. Furthermore, we investigated the relationships between heterotrophic bacterial abundance and riverine DOC or marine DOC. In this study, we assumed that bacterial abundance is representative of bacterial activity, based on the results obtained in previous studies (Kirchman et al., 2009; Maranger et al., 2015; Ortega-Retuerta et al., 2012; Sipler et al., 2017), which suggested that bacterial abundance can be used as a proxy for bacterial activity in the western Arctic.

In the CBL/NCS region, heterotrophic bacterial abundances tended to be high when riverine DOC concentrations were low (Figure 9a). However, the lowest heterotrophic bacterial abundance values were found even at low riverine DOC levels. The opposite trend was observed for the relationship between heterotrophic bacterial abundance and marine DOC concentration (Figure 9b). However, heterotrophic bacterial abundances also had the lowest values at high marine DOC levels. Overall, heterotrophic bacterial abundance showed no relationships

with riverine DOC ($r^2 = 0.0097$, $p > 0.05$, $n = 78$) and marine DOC concentrations ($r^2 = 0.083$, $p < 0.05$, $n = 78$) in the region.

Meanwhile, in the ESS/MR region, the relationships between heterotrophic bacterial abundance and riverine DOC or marine DOC concentrations were unclear (Figures 9d and 9e). In addition, no significant relationships were found between heterotrophic bacterial abundances and Chl-a concentrations in both the CBL/NCS and ESS/MR regions (Figures 9c and 9f).

4. Discussion

4.1. Influence of Hydrographic Features on Riverine and Marine DOC

4.1.1. Riverine DOC

The spatial distribution of riverine DOC showed a clear distinction in its distribution between the CBL/NCS and ESS/MR regions, with higher concentration and contribution in the CBL/NCS region. The contributions of riverine DOC from this study were comparable to previous values reported in the western Arctic Ocean by Guay et al. (1999) (12–56%), Opsahl et al. (1999; 5–22%), and Wheeler et al. (1997%; 25%).

Our research stations in the CBL/NCS region coincide with the position of the edge of convergent Beaufort Gyre, creating conducive conditions for the accumulation of freshwater, strong stratification, a deepening of the nutricline, and a longer residence time (Bluhm et al., 2015; Hansell et al., 2004; Jung, Son, et al., 2021; McLaughlin & Carmack, 2010; Morison et al., 2012; Polyakov et al., 2020). Our observational datasets clearly show these characteristics in the CBL/NCS region. Previous studies (e.g., Guay & Falkner, 1997; Macdonald et al., 1999; Yamamoto-Kawai et al., 2009) revealed that the major fraction of freshwater in the Beaufort Gyre is of Mackenzie River origin, suggesting the influence of the Mackenzie River on riverine DOC in the CBL/NCS region. However, Shen, Benner, et al. (2016) reported that surface distributions of DOC across the Canada Basin (CB) and CBL showed no apparent variation trend (69–73 μM), although the authors observed the influence of the Mackenzie River in the Beaufort Sea (e.g., high concentrations of DOC and lignin phenols). This result suggests that the strong signal of riverine DOC from the Mackenzie River was not detected in the CBL/NCS region, probably due to a decadal residence time in the Beaufort Gyre (Shen, Benner, et al., 2016).

Riverine DOC in river runoff to the western Arctic eventually mixes with older waters that have recirculated within the Beaufort Gyre for a decade (Hansell et al., 2004; Letscher et al., 2011), suggesting that more aged riverine DOC is present in the CBL and CB. Jung, Son, et al. (2021) demonstrated using the fluorescence properties of dissolved organic matter (FDOM) that more aged riverine DOM accumulates within the Beaufort Gyre. The presence of more aged riverine DOC suggests decreases in DOC concentration and the bioavailability of DOM during aging in the water column due to the microbial utilization of bioavailable DOM (Shen et al., 2018). In addition, water column stratification constrains the vertical supply of nutrients to the surface layer, thus leading to very low surface Chl-a concentrations due to highly oligotrophic conditions in summer. Thus, the regional characteristics in the CBL/NCS region, including the accumulation of freshwater, strong stratification, a deepening of the nutricline, and a longer residence time, exerted significant influences on the relatively high riverine DOC concentration, its high contribution, and the lower heterotrophic bacterial abundance in the CBL/NCS region (Figures 7 and 8).

In general, a strong terrestrial origin of DOC has been observed in the surface water of the Arctic Ocean (e.g., Hansell et al., 2004; Letscher et al., 2011; Mathis et al., 2005; Opsahl et al., 1999; Shen, Benner, et al., 2016). However, substantial riverine DOC and f_{rw} but negative f_{sim} values were found in the upper halocline layer, indicating the occurrence of brine rejection from growing sea ice (Yamamoto-Kawai et al., 2005). Similar results were reported in the western Arctic Ocean by Jung, Son, et al. (2021), who found the transport of riverine DOM from the surface to the upper halocline layer by brine rejection from sea ice during winter. Thus, our results support that sea ice formation is a crucial factor in the transport of riverine DOC from the surface to the upper halocline layer in the western Arctic (e.g., Guéguen et al., 2007; Macdonald et al., 2002).

4.1.2. Marine DOC

Contrary to the situation in the CBL/NCS region, high marine DOC concentrations and their contributions were found in the ESS/MR region, especially in the shelf/slope region. The lower concentrations and contributions of marine DOC in the CBL/NCS region can be explained by the relatively stronger influence of river runoff. The high marine DOC concentrations in the ESS/MR region were accompanied by high marine biological activities sustained by nutrient supply from deep layers, indicating the supply of nutrient-rich deep water to the surface (Bluhm et al., 2020; Lewis et al., 2020; Spall et al., 2014; Tremblay et al., 2011). In addition, the higher heterotrophic bacterial abundance values in the upper 50 m of the ESS/MR region suggested the supply of bioavailable DOC induced by high marine biological activities.

It should be noted that the high surface Chl-a and high surface nutrients, especially $NO_2 + NO_3$, concentrations in the ESS/MR region during the summer of 2018 are anomalous hydrographic features. Generally, the surface Chl-a concentrations in the ESS/MR region during the summer are remarkably low, as in the CBL/NCS region, owing to nutrient depletion in the form of NO_3 (Carmack et al., 2006; Codispoti et al., 2005, 2013; Jung, Cho, et al., 2021). However, recent hydrographic changes associated with changes in ocean circulation in response to recent sea ice loss and increased wind mixing have been reported in the Arctic Ocean (e.g., Ardyna & Arrigo, 2020; Polyakov et al., 2017, 2020). Nishino et al. (2008) reported that an east−west contrast in nutrient concentrations on the isohaline surface of $S = 32$ in the western Arctic Ocean, with higher values in the west of the Chukchi Plateau (i.e., the ESS/MR region in this study) than in the east of it. The nutrient supply by the temperature minimum water ($S \approx 32$ psu, near-freezing temperature) from the ESS shelf area was thought to be the main cause of this east-west contrast (Nishino et al., 2013). In addition, similar to our results, Jung, Cho, et al. (2021) reported anomalously high surface Chl-a concentrations in the East Siberian shelf/slope region in the summer of 2017. The authors also observed the lateral intrusions of two bodies of cold halocline water (i.e., low salinity cold water, $S \approx 32$ psu, potential temperature (θ) ≤ -1.5°C; high salinity cold water, $S \approx 34.2$∼34.5 psu, $\theta \approx -1$°C) from the Eurasian marginal seas into the East Siberian shelf break along the shelf slope in 2017. The intrusions of cold halocline waters caused unprecedented shoaling of the nutricline, leading to anomalously high surface phytoplankton blooms in typically highly oligotrophic surface waters in the region (Jung, Cho, et al., 2021). Indeed, the vertical profiles of nutrients in the ESS/MR region during the summer of 2018 indicate shoaling of both the halocline boundary (Figure 8i) and the nutricline (Figures 5 and 6).

In addition to the shoaling of the nutricline by the intrusions of cold halocline waters, the high surface nutrients and Chl-a concentrations in the East Siberian shelf/slope region can be explained by shelfbreak upwelling. During the upwelling event, surface waters above the shelf are driven offshore by upwelling favorable winds (generally easterlies in the Arctic) to be replaced by deeper waters overlying the slope that are drawn onshore (Bluhm et al., 2020). As shown in Figure 6, in the vicinity of the East Siberian shelf/slope region, there were upward sloping isopycnal, and the 24.5 kg m^{-3} isopycnal outcropped. These results reflect that the shelfbreak upwelling occurred in the region, which caused anomalously high surface phytoplankton bloom. On the other hand, in the Chukchi shelf/slope region, the SCM was developed at depths of 30–50 m due to the intense stratification that restricts the upward mixing of nutrients into the euphotic zone.

Recently, Corlett and Pickart (2017) and Li et al. (2019) revealed the year-round existence of a westward-flowing current along the continental slope of the Chukchi Sea. The so-called Chukchi Slope Current is surface-intensified in summer and fall (Li et al., 2019) and transports the nutrient-rich Pacific water from Barrow Canyon to the Chukchi Plateau (Watanabe et al., 2017) or even to the Makarov Basin (Mizobata et al., 2016). This suggests that the pathway of Pacific water in the Arctic Basin is influenced by the Beaufort Gyre circulation pattern (Mizobata et al., 2016). Corlett and Pickart (2017) also reported that the westward-flowing Chukchi Slope Current is intensified under enhanced easterly winds (i.e., the wind paralleling the shelfbreak from the southeast), providing upwelling favorable conditions along the shelfbreak (Spall et al., 2014). Although we do not show the wind conditions during the cruise, Figure 6 obviously shows the occurrence of upwelling in the East Siberian shelf/slope region.

Furthermore, the anomalously high surface Chl-a concentrations by the upwelling events observed in the East Siberian shelf/slope region in 2018 (this study) and 2017 (Jung, Cho, et al., 2021) support the modeling results (Zhang et al., 2020). The field observation and modeling results suggest that the changes in the Beaufort Gyre circulation in 2017 and 2018 (i.e., weakening of the anticyclonic ocean circulation) led to enhanced upwelling

in the region (Zhang et al., 2020). The higher marine biological activities in the East Siberian shelf/slope region most likely resulted from the enhanced supply of nutrients upwelled from the halocline in addition to the uplift of nutrient-rich deep waters by the remained cold halocline waters that intruded in 2017 (Jung, Cho, et al., 2021). Consequently, the large contribution of marine DOC and high heterotrophic bacterial abundance in the ESS/MR region suggest the fresh nature of this marine DOC, which is most likely produced by high marine biological activities.

4.2. Heterotrophic Bacterial Response to Riverine and Marine DOC in the Western Arctic in the Summer of 2018

The remarkably low heterotrophic bacterial abundance in the CBL/NCS region may partially be explained by the low biodegradability of riverine DOC (Sipler et al., 2017) and/or the low nutrient levels in the region. Indeed, the bioavailability of DOM in the Beaufort Sea, indicated by the yields of total dissolved amino acids (TDAA, a proxy for labile organic matter), is low due to the influence of the Mackenzie River, low primary production, and nutrient depletion (Shen et al., 2012, 2018), which limits bacterial growth and production during the summer (Ortega-Retuerta et al., 2012).

However, no relationship was found between heterotrophic bacterial abundance and riverine DOC or marine DOC in the CBL/NCS region (Figure 9). This result is not surprising and can be explained as follows. First, the relationships resulted from heterotrophic bacterial activities in response to a mixture of riverine and marine DOC in seawater, although the contribution of each DOC component to the bulk DOC was different. Second, heterotrophic bacterial abundance is dependent on the bioavailability of DOC (Matsuoka et al., 2015; Moran et al., 2000; Sipler et al., 2017). For example, Spencer et al. (2015) found that more than 50% of DOC in permafrost thaw streams collected in the Russian Arctic in September was bioavailable, while the lability of DOC collected from Alaskan Arctic rivers during summer was <10% (Holmes et al., 2008), suggesting that heterotrophic bacterial activity reacts to the supply of bioreactive DOC regardless of its source (Kaiser et al., 2017; Landa et al., 2014; Sipler et al., 2017).

The relationships obtained in the ESS/MR region were unclear due to anomalously high marine biological activities in the East Siberian shelf/slope region. Phytoplankton directly releases some fixed carbon as a bioreactive DOC during growth and senescence (Carlson & Hansell, 2015). Bioavailable DOC is also produced via sloppy feeding on phytoplankton by zooplankton (Carlson & Hansell, 2015). Thus, we speculate that the highest heterotrophic bacterial abundances, when both riverine and marine DOC concentrations showed moderate values (i.e., 10–15 μM C for riverine DOC and 52–65 μM C for marine DOC) (Figure 9), may have been attributed to the rapid consumption of freshly produced DOC by heterotrophic bacteria.

In addition, the anomalous and high phytoplankton blooms caused by the uplifted upper halocline water by the intrusion of cold halocline waters into the East Siberian shelf/slope region have the potential to remove refractory DOC. Shen & Benner (2018) demonstrated that the addition of highly bioavailable DOC (e.g., glucose) could result in enhanced degradation of more refractory DOC, suggesting that refractory DOC that is resistant to degradation by the microbial community of a given ecosystem can be utilized by microbes of another ecosystem (Baltar et al., 2021). Thus, the supply of nutrients from the deep layer and bioavailable DOC produced by the anomalously high phytoplankton blooms in the East Siberian shelf/slope region likely provides favorable environmental conditions for the degradation of both refractory and riverine DOC as well as bioavailable marine DOC.

It is noteworthy that the simple application of the relationships obtained from this study for the evaluation of the overall response of heterotrophic bacterial activity to riverine and marine DOC would simplify the natural DOC production and consumption processes. Nevertheless, our results show that the Arctic changes associated with ocean circulation, especially in the East Siberian shelf/slope region (Jung, Cho, et al., 2021), have already impacted the marine carbon cycle.

4.3. Comparison With Previous Studies

In this section, we compare our results with previous studies carried out in the western Arctic Ocean. Although there have been few observations for riverine and marine DOC in our study region, we can compare the previously

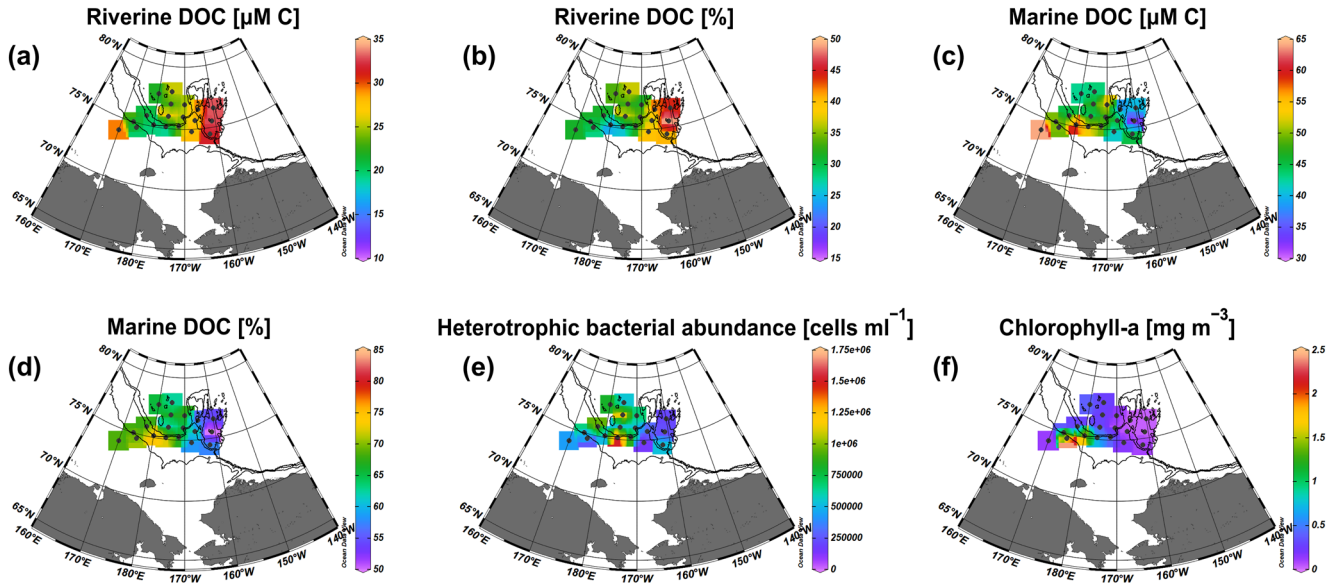

Figure 10. Surface distributions of (a) riverine dissolved organic carbon (DOC) concentration (μM C), (b) contribution of riverine DOC to the observed DOC (%), (c) marine DOC concentration (μM C), (d) contribution of marine DOC to the observed DOC (%), (e) heterotrophic bacterial abundance (cells ml^{-1}), and (f) chlorophyll-a (mg m^{-3}) in the western Arctic during the summer of 2017. Note that (a) and (b) were modified from Jung, Son, et al. (2021). Detailed hydrographic conditions during the 2017 cruise are available in Jung, Son, et al. (2021) and Jung, Cho, et al. (2021). All surface samples were collected at a depth of 3 m. The black contours indicate isobaths of 100, 500, 1,000 m. Figures were illustrated using Ocean Data View software (Schlitzer, 2021).

published data from the IBR/V *Araon* cruise conducted in the summer of 2017 (Jung, Cho, et al., 2021; Jung, Son, et al., 2021).

The results for riverine DOC from 2018 (i.e., this study) were consistent with those obtained in 2017 (Figure 10) by Jung, Son, et al. (2021), who reported higher surface concentrations (mean: 29 ± 4 μM C and range: 24–33 μM C) and contributions (mean: 39 ± 6% and range: 32–49%) of riverine DOC in the CBL/NCS region than those in the ESS/MR region (mean: 23 ± 3 μM C, range: 19–29 μM C, mean: 31 ± 4%, and range: 25–37%). Moreover, the vertical distributions of riverine DOC from 2018 were similar to those found during the summer of 2017, consistent with the DOM fluorescence (i.e., terrestrial humic-like component, a reliable tracer of riverine DOM) distribution (Jung, Son, et al., 2021).

Meanwhile, Shen, Benner, et al. (2016) reported that the mean DOC concentration in surface waters of the CB observed during summer was 69 ± 6 μM (range: 52–88 μM). This value was comparable to our bulk DOC concentration in the CBL/NCS region (mean: 70 ± 3.2 μM C, range: 65–76 μM C). They also reported that vertical distributions of DOC concentrations in the CB and adjacent areas (i.e., CBL, Sever Spur, and Mendeleev Plain) were similar and showed no apparent latitudinal trends (72–83°N, 127–162°W). Thus, the comparable results for DOC between this study (or Jung, Son, et al., 2021) and Shen, Benner, et al. (2016) suggest that similar oceanic conditions influence the CBL/NCS region and the CB and that the measurement of bulk DOC has a limitation to detect the variation in riverine DOC in the region.

There is no evidence of long-term (interannual) accumulation of DOC in the waters over the Chukchi shelf or in the CB (Mathis et al., 2007). This is supported by DeFrancesco and Guéguen (2021), who reported that no interannual variation in bulk DOC concentration was found in the polar mixed layer of the CB over the 11-year (2007–2017) survey. This result suggests that DOC must be remineralized or transported into the deep Arctic Ocean (Mathis et al., 2007). The spatial distributions of riverine and marine DOC from this study provide evidence that the absence of long-term accumulation of DOC is likely caused by the transport of riverine DOC to the upper halocline layer by brine rejection and the relatively fresh nature of marine DOC in the upper water column in the western Arctic Ocean.

We found the highest concentrations and contributions of riverine DOC in the CBL/NCS in 2017 and 2018. However, more substantial influences of continental river runoff and terrigenous DOC than those in the CB were observed in the Makarov Basin, indicating pronounced Siberian river inputs (Shen, Benner, et al., 2016).

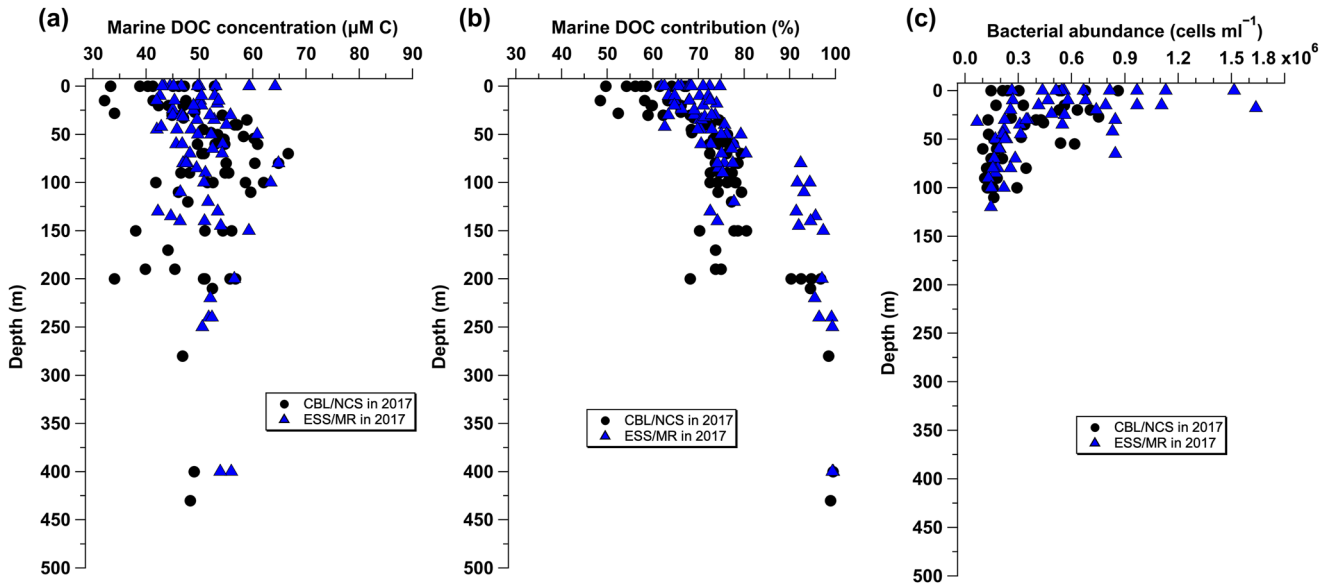

Figure 11. Vertical profiles of (a) marine dissolved organic carbon (DOC) (μM C), (b) marine DOC contribution (%), and (c) bacterial abundance (cells ml^{-1}) observed in the Chukchi Borderland/northern Chukchi Sea (solid black circles) and East Siberian Sea/Mendeleyev Ridge (solid blue triangles) regions in the summer of 2017. Note that the vertical profiles of concentrations and contributions of riverine DOC, river fraction (f_{rw}), and sea-ice meltwater fraction (f_{sim}) observed in the two regions during the 2017 cruise are available in Jung et al. (2021a).

This difference between the two basins is attributed to the position of the Transpolar Drift, which is determined by the Arctic Oscillation, a large-scale Arctic climate pattern (Bauch et al., 2011; Charette et al., 2020; Manizza et al., 2009). Fluvial discharge entrained in the Transpolar Drift is a significant source of terrigenous DOC to surface waters of the central Arctic (Amon, 2004; Letscher et al., 2011; Shen, Benner, et al., 2016). Further research, therefore, is needed to better capture the spatial and temporal variability and the response of riverine DOC to the effects of changing climate on the Arctic Ocean circulation.

Here we report the concentrations and distributions of marine DOC estimated from the 2017 data (Figures 10 and 11) since Jung, Son, et al. (2021) reported only the dynamics of riverine DOC in the western Arctic Ocean. In the summer of 2017, the marine DOC concentration in the surface layer ranged from 33–53 μM C (mean: 44 ± 6 μM C) and 43–64 μM C (mean: 50 ± 7 μM C) in the CBL/NCS and ESS/MR regions, respectively, which were similar to the results from 2018. The mean contributions of marine DOC (mean: 60 ± 6%, range: 50–67% for the CBL/NCS region; mean: 68 ± 4%, range: 62–75% for the ESS/MR region) were comparable to those from 2018 as well.

It is interesting to note that the highest marine DOC concentrations and contributions largely coincided with high biological activities in the shelf/slope region in both 2017 and 2018. As discussed in Section 4.1.2, the lateral intrusions of two bodies of cold halocline water into the ESS/MR region in 2017 resulted in unprecedented shoaling of the nutricline (Jung, Cho, et al., 2021). Also, the shoaling of the nutricline by the remained cold halocline waters was found in 2018. Coincident with shoaling of the nutricline, shelfbreak upwelling appeared to promote the supply of nutrients to the surface layer, thus resulting in the anomalously high surface summer blooms and high marine DOC contribution in the shelf/slope region in both 2017 and 2018. The high bacterial activities accompanied by the anomalously high summer blooms appeared to exert a pronounced influence on the distribution of marine DOC in the study region.

A comparison of the results from 2018 (i.e., this study) with the 2017 data (Figures 10 and 11) reveals several similarities, including the east–west contrast in riverine and marine DOC distributions and higher biological activities in the shelf/slope region. However, the other comparison of our bulk DOC concentrations with those from previous studies provides evidence that distinguishing riverine or marine DOC from bulk DOC is necessary to understand the Arctic DOC cycle more clearly. However, it is worth noting that the extremely high surface marine biological activities and marine DOC contribution in the ESS/MR region in the summers of 2017 and 2018 should be considered anomalous because the surface Chl-a concentrations were extremely low

(0.035–0.26 mg m^{-3}) in the summers of 2011–2016 in our study region (Jung, Cho, et al., 2021). In addition, based on the 2002–2004 and 2008–2010 summer observations (Nishino et al., 2013), the lateral intrusion of high salinity cold water ($S \approx 34.2{\sim}34.5$ psu, $\theta \approx -1°C$) into the East Siberian shelf break along the shelf slope was not observed before 2017 in the ESS/MR region. Given that the seasonal production of marine DOC via primary production is reflected less in bulk DOC concentration (Shen et al., 2012), our results highlight that the shoaling of the nutricline caused by the intrusion of cold halocline waters into the ESS/MR region and prominent shelfbreak upwelling by the poleward retreat of sea-ice edge have altered the marine carbon cycle in the western Arctic Ocean.

5. Conclusions

In this study, we reported the spatial distribution of riverine and marine DOC in the western Arctic Ocean. The regional characteristics in the CBL/NCS region, including the accumulation of freshwater, strong stratification, and the long residence time of water within the anticyclonic Beaufort Gyre, exerted a significant influence on the distribution and concentration of riverine DOC. In comparison, the anomalous and high phytoplankton blooms caused by the uplifted upper halocline water by the intrusion of cold halocline waters into the East Siberian shelf/slope region enhanced the production of marine DOC and the bioavailability of DOC. It is worth noting that the spatial distributions of freshwater components and riverine and marine DOC in the western Arctic were investigated during a limited sampling period. Thus, our results should be considered representative of those throughout the sampling period only.

As previous studies (Jung, Cho, et al., 2021; Polyakov et al., 2017, 2020) revealed, the Arctic Ocean is experiencing radical modification in its hydrographic properties and overall circulation (Ardyna & Arrigo, 2020). Our results clearly highlight that the shoaling of the nutricline with consequences for high marine biological activities by shelfbreak upwelling has already impacted the Arctic marine carbon cycle, especially in the ESS/MR region. In addition, the retreat of the ice edge beyond the shelf break will provide upwelling favorable conditions along the shelf break (Carmack & Chapman, 2003), with increasing seasonal production of marine DOC. Moreover, the intense loss of multi-year sea ice (Cavalieri & Parkinson, 2012; Perovich et al., 2020) will most likely increase carbon export to the ocean's deeper layers (Jung, Son, et al., 2021). Furthermore, recent warming temperatures (Ballinger et al., 2020) and consequent permafrost thaw (Abbott et al., 2016) in the Arctic Ocean will induce alterations in the quantity and distribution of riverine DOC with dramatic consequences for Arctic biogeochemical cycles. Hence, further research is necessary to elucidate temporal and spatial variation trends of marine and riverine DOC and analyze the changes that affect the Arctic marine ecosystem.

Conflict of Interest

The authors declare no conflicts of interest relevant to this study.

Data Availability Statement

All data are available on the KOPRI data servers accessible through https://dx.doi.org/doi:10.22663/KOPRI-KPDC-00001659.1.

Acknowledgments
We are grateful to the captain and crew of the IBR/V *Araon* for their enthusiastic assistance during the ARA09B cruise. This research was a part of the project titled "Korea-Arctic Ocean Warming and Response of Ecosystem (K-AWARE)", the Korea Polar Research Institute (KOPRI) 1525011760, funded by the Ministry of Oceans and Fisheries, Korea.

References

Årthun, M., Onarheim, I. H., Dörr, J., & Eldevik, T. (2021). The seasonal and regional transition to an ice-free Arctic. *Geophysical Research Letters*, *48*(1), e2020GL090825. https://doi.org/10.1029/2020GL090825

Abbott, B. W., Jones, J. B., Schuur, E. A. G., Chapin, F. S., III, Bowden, W. B., Bret-Harte, M. S., et al. (2016). Biomass offsets little or none of permafrost carbon release from soils, streams, and wildfire: An expert assessment. *Environmental Research Letters*, *11*(3), 034014. https://doi.org/10.1088/1748-9326/11/3/034014

Abbott, B. W., Larouche, J. R., Jones, J. B., Bowden, W. B., & Balser, A. W. (2014). Elevated dissolved organic carbon biodegradability from thawing and collapsing permafrost. *Journal of Geophysical Research: Biogeosciences*, *119*(10), 2049–2063. https://doi.org/10.1002/2014JG002678

Alkire, M. B., Rember, R., & Polyakov, I. (2019). Discrepancy in the identification of the Atlantic/Pacific front in the central Arctic Ocean: NO versus nutrient relationships. *Geophysical Research Letters*, *46*(7), 3843–3852. https://doi.org/10.1029/2018GL081837

Alling, V., Sanchez-Garcia, L., Porcelli, D., Pugach, S., Vonk, J. E., van Dongen, B., et al. (2010). Nonconservative behavior of dissolved organic carbon across the Laptev and East Siberian seas. *Global Biogeochemical Cycles*, *24*(4), GB4033. https://doi.org/10.1029/2010GB003834

Amon, R. M. W. (2004). The role of dissolved organic matter for the organic carbon cycle in the Arctic Ocean. In R. Stein & R. W. Macdonald (Eds.), *The organic carbon cycle in the Arctic Ocean* (pp. 83–99). Springer.

Amon, R. M. W., & Meon, B. (2004). The biogeochemistry of dissolved organic matter and nutrients in two large Arctic estuaries and potential implications for our understanding of the Arctic Ocean system. *Marine Chemistry*, *92*(1–4), 311–330. https://doi.org/10.1016/j.marchem.2004.06.034

Anderson, L. G., & Amon, R. M. W. (2015). DOM in the Arctic Ocean. In D. A. Hansell & C. A. Carlson (Eds.), *Biogeochemistry of marine dissolved organic matter* (2nd ed., pp. 609–633). Academic Press.

Ardyna, M., & Arrigo, K. R. (2020). Phytoplankton dynamics in a changing Arctic Ocean. *Nature Climate Change*, *10*, 892–903. https://doi.org/10.1038/s41558-020-0905-y

Arrigo, K. R., & van Dijken, G. L. (2011). Secular trends in Arctic Ocean net primary production. *Journal of Geophysical Research*, *116*(C9), C09011. https://doi.org/10.1029/2011JC007151

Arrigo, K. R., & van Dijken, G. L. (2015). Continued increases in Arctic Ocean primary production. *Progress in Oceanography*, *136*, 60–70. https://doi.org/10.1016/j.pocean.2015.05.002

Ballinger, T. J., Overland, J. E., Wang, M., Bhatt, U. S., Hanna, E., Hanssen-Bauer, I., et al. (2020). Surface air temperature [in NOAA Arctic Report Card 2020]. Retrieved from https://www.arctic.noaa.gov/Report-Card

Baltar, F., Alvarez-Salgado, X. A., Arístegui, J., Benner, R., Hansell, D. A., Herndl, G. J., & Lønborg, C. (2021). What is refractory organic matter in the ocean? *Frontiers in Marine Science*, *8*, 642637. https://doi.org/10.3389/fmars.2021.642637

Bauch, D. (1995). *The distribution of $\delta^{18}O$ in the Arctic Ocean: Implications for the freshwater balance of the halocline and the sources of deep and bottom waters. Reports on Polar Research No. 159* (pp. 1–144). AWI.

Bauch, D., van der Loeff, M. R., Andersen, N., Torres-Valdés, S., Bakker, K., & Abrahamsen, E. P. (2011). Origin of freshwater and polynya water in the Arctic Ocean halocline in summer 2007. *Progress in Oceanography*, *91*(4), 482–495. https://doi.org/10.1016/j.pocean.2011.07.017

Beaupré, S. R. (2015). The carbon isotopic composition of marine DOC. In D. A. Hansell & C. A. Carlson (Eds.), *Biogeochemistry of marine dissolved organic matter* (2nd ed., pp. 335–368). Academic Press.

Benner, R., Louchouarn, P., & Amon, R. M. W. (2005). Terrigenous dissolved organic matter in the Arctic Ocean and its transport to surface and deep waters of the North Atlantic. *Global Biogeochemical Cycles*, *19*(2), GB2025. https://doi.org/10.1029/2004GB002398

Bluhm, B. A., Janout, M. A., Danielson, S. L., Ellingsen, I., Gavrilo, M., Grebmeier, J. M., et al. (2020). The Pan-Arctic continental slope: Sharp gradients of physical processes affect pelagic and benthic ecosystems. *Frontiers in Marine Science*, *7*, 544386. https://doi.org/10.3389/fmars.2020.544386

Bluhm, B. A., Kosobokova, K. N., & Carmack, E. C. (2015). A tale of two basins: An integrated physical and biological perspective of the deep Arctic Ocean. *Progress in Oceanography*, *139*, 89–121. https://doi.org/10.1016/j.pocean.2015.07.011

Buchan, A., LeCleir, G. R., Gulvik, C. A., & González, J. M. (2014). Master recyclers: Features and functions of bacteria associated with phytoplankton blooms. *Nature Reviews Microbiology*, *12*(10), 686–698. https://doi.org/10.1038/nrmicro3326

Carlson, C. A., & Hansell, D. A. (2015). DOM sources, sinks, reactivity, and budgets. In D. A. Hansell & C. A. Carlson (Eds.), *Biogeochemistry of marine dissolved organic matter* (2nd ed., pp. 65–126). Academic Press.

Carmack, E., Barber, D., Christensen, J., Macdonald, R., Rudels, B., & Sakshaug, E. (2006). Climate variability and physical forcing of the food webs and the carbon budget on panarctic shelves. *Progress in Oceanography*, *71*(2–4), 145–181. https://doi.org/10.1016/j.pocean.2006.10.005

Carmack, E., & Chapman, D. C. (2003). Wind-driven shelf/basin exchange on an Arctic shelf: The joint roles of ice cover extent and shelf-break bathymetry. *Geophysical Research Letters*, *30*(14), 1778. https://doi.org/10.1029/2003GL017526

Cavalieri, D. J., & Parkinson, C. L. (2012). Arctic sea ice variability and trends. *The Cryosphere*, *6*(4), 881–889. https://doi.org/10.5194/tc-6-881-2012

Charette, M. A., Kipp, L. E., Jensen, L. T., Dabrowski, J. S., Whitmore, L. M., Fitzsimmons, J. N., et al. (2020). The Transpolar Drift as a source of riverine and shelf-derived trace elements to the Central Arctic Ocean. *Journal of Geophysical Research: Oceans*, *125*(5), e2019JC015920. https://doi.org/10.1029/2019JC015920

Chen, M., Jung, J., Lee, Y. K., & Hur, J. (2018). Surface accumulation of low molecular weight dissolved organic matter in surface waters and horizontal off-shelf spreading of nutrients and humic-like fluorescence in the Chukchi Sea of the Arctic Ocean. *Science of the Total Environment*, *639*, 624–632. https://doi.org/10.1016/j.scitotenv.2018.05.205

Coble, P. G. (1996). Characterization of marine and terrestrial DOM in seawater using excitation-emission matrix spectroscopy. *Marine Chemistry*, *51*(4), 325–346. https://doi.org/10.1016/0304-4203(95)00062-3

Coble, P. G. (2007). Marine optical biogeochemistry: The chemistry of ocean color. *Chemical Reviews*, *107*(2), 402–418. https://doi.org/10.1021/cr050350+

Codispoti, L. A., Flagg, C., Kelly, V., & Swift, J. H. (2005). Hydrographic conditions during the 2002 SBI process experiments. *Deep-Sea Research Part II*, *52*(24–26), 3199–3226. https://doi.org/10.1016/j.dsr2.2005.10.007

Codispoti, L. A., Kelly, V., Thessen, A., Matrai, P., Suttles, S., Hill, V., et al. (2013). Synthesis of primary production in the Arctic Ocean: III. Nitrate and phosphate based estimates of net community production. *Progress in Oceanography*, *110*, 126–150. https://doi.org/10.1016/j.pocean.2012.11.006

Comiso, J. C., Meier, W. N., & Gersten, R. (2017). Variability and trends in the Arctic Sea ice cover: Results from different techniques. *Journal of Geophysical Research: Oceans*, *122*(8), 6883–6900. https://doi.org/10.1002/2017JC012768

Cooper, L. W., Benner, R., McClelland, J. W., Peterson, B. J., Holmes, R. M., Raymond, P. A., et al. (2005). Linkages among runoff, dissolved organic carbon, and the stable oxygen isotope composition of seawater and other water mass indicators in the Arctic Ocean. *Journal of Geophysical Research*, *110*(G2), G02013. https://doi.org/10.1029/2005JG000031

Cooper, L. W., Frey, K. E., Logvinova, C., Biasatti, D. M., & Grebmeier, J. M. (2016). Variations in the proportions of melted sea ice and runoff in surface waters of the Chukchi Sea: A retrospective analysis, 1990–2012, and analysis of the implications of melted sea ice in an under-ice bloom. *Deep-Sea Research Part II*, *130*, 6–13. https://doi.org/10.1016/j.dsr2.2016.04.014

Cooper, L. W., McClelland, J. W., Holmes, R. M., Raymond, P. A., Gibson, J. J., Guay, C. K., & Peterson, B. J. (2008). Flow-weighted values of runoff tracers ($\delta^{18}O$, DOC, Ba, alkalinity) from the six largest Arctic rivers. *Geophysical Research Letters*, *35*(18), L18606. https://doi.org/10.1029/2008GL035007

Corlett, W. B., & Pickart, R. S. (2017). The Chukchi slope current. *Progress in Oceanography*, *153*, 50–65. https://doi.org/10.1016/j.pocean.2017.04.005

Davis, J., & Benner, R. (2005). Seasonal trends in the abundance, composition and bioavailability of particulate and dissolved organic matter in the Chukchi/Beaufort Seas and western Canada Basin. *Deep-Sea Research Part II*, *52*(24–26), 3396–3410. https://doi.org/10.1016/j.dsr2.2005.09.006

DeFrancesco, C., & Guéguen, C. (2021). Long-term trends in dissolved organic matter composition and its relation to sea ice in the Canada Basin, Arctic Ocean (2007–2017). *Journal of Geophysical Research: Oceans*, *126*(2), e2020JC016578. https://doi.org/10.1029/2020JC016578

Dittmar, T., & Kattner, G. (2003). The biogeochemistry of the river and shelf ecosystem of the Arctic Ocean: A review. *Marine Chemistry*, *83*(3–4), 103–120. https://doi.org/10.1016/S0304-4203(03)00105-1

Eicken, H., Krouse, H. R., Kadko, D., & Perovich, D. K. (2002). Tracer studies of pathways and rates of meltwater transport through Arctic summer sea ice. *Journal of Geophysical Research*, *107*(C10), 8046. https://doi.org/10.1029/2000JC000583

Ekwurzel, B., Schlosser, P., Mortlock, R. A., Fairbanks, R. G., & Swift, J. H. (2001). River runoff, sea ice meltwater, and Pacific water distribution and mean residence times in the Arctic Ocean. *Journal of Geophysical Research*, *106*(C5), 9075–9092. https://doi.org/10.1029/1999jc000024

Frey, K. E., & McClelland, J. W. (2009). Impacts of permafrost degradation on arctic river biogeochemistry. *Hydrological Processes*, *23*(1), 169–182. https://doi.org/10.1002/hyp.7196

Giannelli, V., Thomas, D. N., Haas, C., Kattner, G., Kennedy, H., & Dieckmann, G. S. (2001). Behaviour of dissolved organic matter and inorganic nutrients during experimental sea-ice formation. *Annals of Glaciology*, *33*, 317–321. https://doi.org/10.3189/172756401781818572

Goncalves-Araujo, R., Granskog, M. A., Bracher, A., Azetsu-Scott, K., Dodd, P. A., & Stedmon, C. A. (2016). Using fluorescent dissolved organic matter to trace and distinguish the origin of Arctic surface waters. *Scientific Reports*, *6*(1), 33978. https://doi.org/10.1038/srep33978

Gordon, L. I., Jennings, J. C., Jr., Ross, A. A., & Krest, J. M. (1993). A suggested protocol for continuous automated analysis of seawater nutrients (phosphate, nitrate, nitrite and silicic acid) in the WOCE Hydrographic Program and the Joint Global Ocean Fluxes Study. In *WOCE Operations Manual, Volume 3, Section 3.1, Part 3.1.3 WHP Operations and Methods, WHP Office Report WHPO 91-1, WOCE Report No. 68/91, Nov. 1994, Revision 1*. (55 p.). Woods Hole.

Guay, C. K., & Falkner, K. K. (1997). Barium as a tracer of Arctic halocline and river waters. *Deep-Sea Research Part II*, *44*(8), 1543–1569. https://doi.org/10.1016/S0967-0645(97)00066-0

Guay, C. K., Klinkhammer, G. P., Falkner, K. K., Benner, R., Coble, P. G., Whitledge, T. E., et al. (1999). High-resolution measurements of dissolved organic carbon in the Arctic Ocean by in situ fiber-optic spectrometry. *Geophysical Research Letters*, *26*(8), 1007–1010. https://doi.org/10.1029/1999GL900130

Guéguen, C., Guo, L., Yamamoto-Kawai, M., & Tanaka, N. (2007). Colored dissolved organic matter dynamics across the shelf-basin interface in the western Arctic Ocean. *Journal of Geophysical Research*, *112*(C5), C05038. https://doi.org/10.1029/2006JC003584

Guéguen, C., McLaughlin, F. A., Carmack, E. C., Itoh, M., Narita, H., & Nishino, S. (2012). The nature of colored dissolved organic matter in the southern Canada Basin and East Siberian Sea. *Deep-Sea Research Part II*, *81–84*, 102–113. https://doi.org/10.1016/j.dsr2.2011.05.004

Hansell, D. A., Carlson, C. A., Repeta, D. J., & Schlitzer, R. (2009). Dissolved organic matter in the ocean: A controversy stimulates new insights. *Oceanography*, *22*(4), 202–211. https://doi.org/10.2307/24861036

Hansell, D. A., Kadko, D., & Bates, N. R. (2004). Degradation of terrigenous dissolved organic carbon in the western Arctic Ocean. *Science*, *304*(5672), 858–861. https://doi.org/10.1126/science.1096175

Holmes, R. M., McClelland, J. W., Peterson, B. J., Tank, S. E., Bulygina, E., Eglinton, T. I., et al. (2012). Seasonal and annual fluxes of nutrients and organic matter from large rivers to the Arctic Ocean and surrounding seas. *Estuaries and Coasts*, *35*(2), 369–382. https://doi.org/10.1007/s12237-011-9386-6

Holmes, R. M., McClelland, J. W., Raymond, P. A., Frazer, B. B., Peterson, B. J., & Stieglitz, M. (2008). Lability of DOC transported by Alaskan rivers to the Arctic Ocean. *Geophysical Research Letters*, *35*(3), L03402. https://doi.org/10.1029/2007GL032837

Jiao, N., Herndl, G. J., Hansell, D. A., Benner, R., Kattner, G., Wilhelm, S. W., et al. (2010). Microbial production of recalcitrant dissolved organic matter: Long-term carbon storage in the Global Ocean. *Nature Reviews Microbiology*, *8*, 1–7. https://doi.org/10.1038/nrmicro2386

Jung, J., Cho, K.-H., Park, T., Yoshizawa, E., Lee, Y., Yang, E. J., et al. (2021). Atlantic-origin cold saline water intrusion and shoaling of the nutricline in the Pacific Arctic. *Geophysical Research Letters*, *48*(6), e2020GL090907. https://doi.org/10.1029/2020GL090907

Jung, J., Son, J. E., Lee, Y. K., Cho, K.-H., Lee, Y., Yang, E. J., et al. (2021). Tracing riverine dissolved organic carbon and its transport to the halocline layer in the Chukchi Sea (western Arctic Ocean) using humic-like fluorescence fingerprinting. *Science of the Total Environment*, *772*, 145542. https://doi.org/10.1016/j.scitotenv.2021.1455

Kaiser, K., Canedo-Oropeza, M., McMahon, R., & Amon, R. M. W. (2017). Origins and transformations of dissolved organic matter in large Arctic rivers. *Scientific Reports*, *7*(1), 13064. https://doi.org/10.1038/s41598-017-12729-1

Kattner, G., Lobbes, J. M., Fitznar, H. P., Engbrodt, R., Nöthig, E. M., & Lara, R. J. (1999). Tracing dissolved organic substances and nutrients from the Lena River through Laptev Sea (Arctic). *Marine Chemistry*, *65*(1–2), 25–39. https://doi.org/10.1016/S0304-4203(99)00008-0

Kirchman, D. L., Hill, V., Cottrell, M. T., Gradinger, R., Malmstrom, R. R., & Parker, A. (2009). Standing stocks, production, and respiration of phytoplankton and heterotrophic bacteria in the western Arctic Ocean. *Deep-Sea Research Part II*, *56*(17), 1237–1248. https://doi.org/10.1016/j.dsr2.2008.10.018

Landa, M., Cottrell, M. T., Kirchman, D. L., Kaiser, K., Medeiros, P. M., Tremblay, L., et al. (2014). Phylogenetic and structural response of heterotrophic bacteria to dissolved organic matter of different chemical composition in a continuous culture study. *Environmental Microbiology*, *16*(6), 1668–1681. https://doi.org/10.1111/1462-2920.12242

Lechtenfeld, O. J., Hertkorn, N., Shen, Y., Witt, M., & Benner, R. (2015). Marine sequestration of carbon in bacterial metabolites. *Nature Communications*, *6*(1), 6711. https://doi.org/10.1038/ncomms7711

Lee, Y., Min, J.-O., Yang, E. J., Cho, K.-H., Jung, J., Park, J., et al. (2019). Influence of sea ice concentration on phytoplankton community structure in the Chukchi and East Siberian Seas, Pacific Arctic Ocean. *Deep-Sea Research Part I*, *147*, 54–64. https://doi.org/10.1016/j.dsr.2019.04.001

Le Fouest, V., Matsuoka, A., Manizza, M., Shernetsky, M., Tremblay, B., & Babin, M. (2018). Towards an assessment of riverine dissolved organic carbon in surface waters of the western Arctic Ocean based on remote sensing and biogeochemical modeling. *Biogeosciences*, *15*(5), 1335–1346. https://doi.org/10.5194/bg-15-1335-2018

Letscher, R. T., Hansell, D. A., & Kadko, D. (2011). Rapid removal of terrigenous dissolved organic carbon over the Eurasian shelves of the Arctic Ocean. *Marine Chemistry*, *123*(1–4), 78–87. https://doi.org/10.1016/j.marchem.2010.10.002

Lewis, K. M., van Dijken, G. L., & Arrigo, K. R. (2020). Changes in phytoplankton concentration now drive increased Arctic Ocean primary production. *Science*, *369*(6500), 198–202. https://doi.org/10.1126/science.aay8380

Li, M., Pickart, R. S., Spall, M. A., Weingartner, T. J., Lin, P., Moore, G. W. K., & Qi, Y. (2019). Circulation of the Chukchi Sea shelfbreak and slope from moored timeseries. *Progress in Oceanography*, *172*, 14–33. https://doi.org/10.1016/j.pocean.2019.01.002

Lobbes, J. M., Fitznar, H. P., & Kattner, G. (2000). Biogeochemical characteristics of dissolved and particulate organic matter in Russian rivers entering the Arctic Ocean. *Geochimica et Cosmochimica Acta*, *64*(17), 2973–2983. https://doi.org/10.1016/S0016-7037(00)00409-9

Logvinova, C. L., Frey, K. E., & Cooper, L. W. (2016). The potential role of sea ice melt in the distribution of chromophoric dissolved organic matter in the Chukchi and Beaufort Seas. *Deep-Sea Research Part II*, *130*, 28–42. https://doi.org/10.1016/j.dsr2.2016.04.017

Lønborg, C., Carreira, C., Jickells, T., & Álvarez-Salgado, X. A. (2020). Impacts of global change on ocean dissolved organic carbon (DOC) cycling. *Frontiers in Marine Science*, *7*, 466. https://doi.org/10.3389/fmars.2020.00466

Macdonald, R. W., Carmack, E. C., McLaughlin, F. A., Falkner, K. K., & Swift, J. H. (1999). Connections among ice, runoff and atmospheric forcing in the Beaufort Gyre. *Geophysical Research Letters*, *26*(15), 2223–2226. https://doi.org/10.1029/1999GL900508

Macdonald, R. W., McLaughlin, F. A., & Carmack, E. C. (2002). Fresh water and its sources during the SHEBA drift in the Canada Basin of the Arctic Ocean. *Deep-Sea Research Part I*, *49*(10), 1769–1785. https://doi.org/10.1016/S0967-0637(02)00097-3

Manizza, M., Follows, M. J., Dutkiewicz, S., McClelland, J. W., Menemenlis, D., Hill, C. N., et al. (2009). Modeling transport and fate of riverine dissolved organic carbon in the Arctic Ocean. *Global Biogeochemical Cycles*, *23*(4), GB4006. https://doi.org/10.1029/2008GB003396

Mann, P. J., Davydova, A., Zimov, N., Spencer, R. G. M., Davydov, S., Bulygina, E., et al. (2012). Controls on the composition and lability of dissolved organic matter in Siberia's Kolyma River basin. *Journal of Geophysical Research*, *117*(G1), G01028. https://doi.org/10.1029/2011JG001798

Maranger, R., Vaqué, D., Nguyen, D., Hébert, M.-P., & Lara, E. (2015). Pan-Arctic patterns of planktonic heterotrophic microbial abundance and processes: Controlling factors and potential impacts of warming. *Progress in Oceanography*, *139*, 221–232. https://doi.org/10.1016/j.pocean.2015.07.006

Marie, D., Partensky, F., Jacquet, S., & Vaulot, D. (1997). Enumeration and cell cycle analysis of natural populations of marine picoplankton by flow cytometry using the nucleic acid stain SYBR Green I. *Applied and Environmental Microbiology*, *63*(1), 186–193. https://doi.org/10.1128/aem.63.1.186-193.1997

Mathis, J. T., Bates, N. R., Hansell, D. A., & Babila, T. (2009). Net community production in the northeastern Chukchi Sea. *Deep-Sea Research Part II*, *56*(17), 1213–1222. https://doi.org/10.1016/j.dsr2.2008.10.017

Mathis, J. T., Hansell, D. A., & Bates, N. R. (2005). Strong hydrographic controls on spatial and seasonal variability of dissolved organic carbon in the Chukchi Sea. *Deep-Sea Research Part II*, *52*(24–26), 3245–3258. https://doi.org/10.1016/j.dsr2.2005.10.002

Mathis, J. T., Hansell, D. A., Kadko, D., Bates, N. R., & Cooper, L. W. (2007). Determining net dissolved organic carbon production in the hydrographically complex western Arctic Ocean. *Limnology & Oceanography*, *52*(5), 1789–1799. https://doi.org/10.4319/lo.2007.52.5.1789

Matsuoka, A., Ortega-Retuerta, E., Bricaud, A., Arrigo, K. R., & Babin, M. (2015). Characteristics of colored dissolved organic matter (CDOM) in the Western Arctic Ocean: Relationships with microbial activities. *Deep-Sea Research Part II*, *118*, 44–52. https://doi.org/10.1016/j.dsr2.2015.02.012

McClelland, J. W., Holmes, R. M., Dunton, K. H., & Macdonald, R. W. (2012). The Arctic Ocean Estuary. *Estuaries and Coasts*, *35*(2), 353–368. https://doi.org/10.1007/s12237-010-9357-3

McGuire, A. D., Anderson, L. G., Christensen, T. R., Dallimore, S., Guo, L., Hayes, D. J., et al. (2009). Sensitivity of the carbon cycle in the Arctic to climate change. *Ecological Monographs*, *79*(4), 523–555. https://doi.org/10.1890/08-2025.1

McLaughlin, F. A., & Carmack, E. C. (2010). Deepening of the nutricline and chlorophyll maximum in the Canada Basin interior, 2003–2009. *Geophysical Research Letters*, *37*(24), L24602. https://doi.org/10.1029/2010GL045459

Mizobata, K., Watanabe, E., & Kimura, N. (2016). Wintertime variability of the Beaufort Gyre in the Arctic Ocean derived from CryoSat-2/SIRAL observations. *Journal of Geophysical Research: Oceans*, *121*(3), 1685–1699. https://doi.org/10.1002/2015JC011218

Moran, M. A., Sheldon, W. M., Jr., & Zepp, R. G. (2000). Carbon loss and optical property changes during long-term photochemical and biological degradation of estuarine dissolved organic matter. *Limnology & Oceanography*, *45*(6), 1254–1264. https://doi.org/10.4319/lo.2000.45.6.1254

Morison, J., Kwok, R., Peralta-Ferriz, C., Alkire, M., Rigor, I., Andersen, R., & Steele, M. (2012). Changing Arctic Ocean freshwater pathways. *Nature*, *481*(7379), 66–70. https://doi.org/10.1038/nature10705

Nishino, S., Itoh, M., Williams, W. J., & Semiletov, I. (2013). Shoaling of the nutricline with an increase in near-freezing temperature water in the Makarov Basin. *Journal of Geophysical Research: Oceans*, *118*(2), 635–649. https://doi.org/10.1029/2012JC008234

Nishino, S., Shimada, K., Itoh, M., Yamamoto-Kawai, M., & Chiba, S. (2008). East–west differences in water mass, nutrient, and chlorophyll a distributions in the sea ice reduction region of the western Arctic Ocean. *Journal of Geophysical Research*, *113*, C00A01. https://doi.org/10.1029/2007JC004666

Ogawa, H., Amagai, Y., Koike, I., Kaiser, K., & Benner, R. (2001). Production of refractory dissolved organic matter by bacteria. *Science*, *292*(5518), 917–920. https://doi.org/10.1126/science.1057627

Opsahl, S., Benner, R., & Amon, R. M. W. (1999). Major flux of terrigenous dissolved organic matter through the Arctic Ocean. *Limnology & Oceanography*, *44*(8), 2017–2023. https://doi.org/10.4319/lo.1999.44.8.2017

Ortega-Retuerta, E., Jeffrey, W. H., Babin, M., Bélanger, S., Benner, R., Marie, D., et al. (2012). Carbon fluxes in the Canadian Arctic: Patterns and drivers of bacterial abundance, production and respiration on the Beaufort Sea margin. *Biogeosciences*, *9*, 3679–3692. https://doi.org/10.5194/bg-9-3679-2012

Pan, L. A., Zhang, L. H., Zhang, J., Gasol, J. M., & Chao, M. (2005). On-board flow cytometric observation of picoplankton community structure in the East China Sea during the fall of different years. *FEMS Microbiology Ecology*, *52*(2), 243–253. https://doi.org/10.1016/j.femsec.2004.11.019

Perovich, D., Meier, W., Tschudi, T., Hendricks, S., Petty, A. A., Divine, D., et al. (2020). Sea Ice [in NOAA Arctic Report Card 2020]. Retrieved from https://www.arctic.noaa.gov/Report-Card

Peterson, B. J., Holmes, R. M., McClelland, J. W., Vörösmarty, C. J., Lammers, R. B., Shiklomanov, A. I., et al. (2002). Increasing river discharge to the Arctic Ocean. *Science*, *298*(5601), 2171–2173. https://doi.org/10.1126/science.1077445

Pfirman, S., Haxby, W., Eicken, H., Jeffries, M., & Bauch, D. (2004). Drifting Arctic sea ice archives changes in ocean surface conditions. *Geophysical Research Letters*, *31*(19), L19401. https://doi.org/10.1029/2004GL020666

Polyakov, I. V., Alkire, M. B., Bluhm, B. A., Brown, K. A., Carmack, E. C., Chierici, M., et al. (2020). Borealization of the Arctic Ocean in response to anomalous advection from sub-Arctic seas. *Frontiers in Marine Science*, *7*, 491. https://doi.org/10.3389/fmars.2020.00491

Polyakov, I. V., Pnyushkov, A. V., Alkire, M. B., Ashik, I. M., Baumann, T. M., Carmack, E. C., et al. (2017). Greater role for Atlantic inflows on sea-ice loss in the Eurasian Basin of the Arctic Ocean. *Science*, *356*(6335), 285–291. https://doi.org/10.1126/science.aai8204

Raymond, P. A., McClelland, J. W., Holmes, R. M., Zhulidov, A. V., Mull, K., Peterson, B. J., et al. (2007). Flux and age of dissolved organic carbon exported to the Arctic Ocean: A carbon isotopic study of the five largest arctic rivers. *Global Biogeochemical Cycles*, *21*(4), GB4011. https://doi.org/10.1029/2007GB002934

Raymond, P. A., & Spencer, R. G. M. (2015). Riverine DOC. In D. A. Hansell & C. A. Carlson (Eds.), *Biogeochemistry of marine dissolved organic matter* (2nd ed., pp. 509–533). Academic Press.

Schlitzer, R. (2021). Ocean Data View. Retrieved from http://odv.awi.de

Schuur, E. A. G., McGuire, A. D., Schaedel, C., Grosse, G., Harden, J. W., Hayes, D. J., et al. (2015). Climate change and the permafrost carbon feedback. *Nature*, *520*(7546), 171–179. https://doi.org/10.1038/nature14338

Shen, Y., & Benner, R. (2018). Mixing it up in the ocean carbon cycle and the removal of refractory dissolved organic carbon. *Scientific Reports*, *8*(1), 1–9. https://doi.org/10.1038/s41598-018-20857-5

Shen, Y., Benner, R., Kaiser, K., Fichot, C. G., & Whitledge, T. E. (2018). Pan-Arctic distribution of bioavailable dissolved organic matter and linkages with productivity in ocean margins. *Geophysical Research Letters*, *45*(3), 1490–1498. https://doi.org/10.1002/2017GL076647

Shen, Y., Benner, R., Robbins, L. L., & Wynn, J. G. (2016). Sources, distributions, and dynamics of dissolved organic matter in the Canada and Makarov Basins. *Frontiers in Marine Science*, *3*, 198. https://doi.org/10.3389/fmars.2016.00198

Shen, Y., Fichot, C. G., & Benner, R. (2012). Dissolved organic matter composition and bioavailability reflect ecosystem productivity in the Western Arctic Ocean. *Biogeosciences*, *9*(12), 4993–5005. https://doi.org/10.5194/bg-9-4993-2012

Shen, Y., Fichot, C. G., Liang, S.-K., & Benner, R. (2016). Biological hot spots and the accumulation of marine dissolved organic matter in a highly productive ocean margin. *Limnology & Oceanography*, *61*(4), 1287–1300. https://doi.org/10.1002/lno.10290

Sipler, R. E., Kellogg, C. T. E., Connelly, T. L., Roberts, Q. N., Yager, P. L., & Bronk, D. A. (2017). Microbial community response to terrestrially derived dissolved organic matter in the coastal Arctic. *Frontiers in Microbiology*, *8*, 1018. https://doi.org/10.3389/fmicb.2017.01018

Spall, M. A., Pickart, R. S., Brugler, E. T., Moore, G. W. K., Thomas, L., & Arrigo, K. R. (2014). Role of shelfbreak upwelling in the formation of a massive under-ice bloom in the Chukchi Sea. *Deep-Sea Research Part II*, *105*, 17–29. https://doi.org/10.1016/j.dsr2.2014.03.017

Spencer, R. G. M., Mann, P. J., Dittmar, T., Eglinton, T. I., McIntyre, C., Holmes, R. M., et al. (2015). Detecting the signature of permafrost thaw in Arctic rivers. *Geophysical Research Letters*, *42*(8), 2830–2835. https://doi.org/10.1002/2015GL063498

Stedmon, C. A., Amon, R. M. W., Rinehart, A. J., & Walker, S. A. (2011). The supply and characteristics of colored dissolved organic matter (CDOM) in the Arctic Ocean: Pan arctic trends and differences. *Marine Chemistry*, *124*(1–4), 108–118. https://doi.org/10.1016/j.marchem.2010.12.007

Stedmon, C. A., Markager, S., & Bro, R. (2003). Tracing dissolved organic matter in aquatic environments using a new approach to fluorescence spectroscopy. *Marine Chemistry*, *82*(3–4), 239–254. https://doi.org/10.1016/S0304-4203(03)00072-0

Tanaka, K., Takesue, N., Nishioka, J., Kondo, Y., Ooki, A., Kuma, K., et al. (2016). The conservative behavior of dissolved organic carbon in surface waters of the southern Chukchi Sea, Arctic Ocean, during early summer. *Scientific Reports*, *6*(1), 34123. https://doi.org/10.1038/srep34123

Thomas, D. N., Kattner, G., Engbrodt, R., Giannelli, V., Kennedy, H., Haas, C., & Dieckmann, G. S. (2001). Dissolved organic matter in Antarctic sea ice. *Annals of Glaciology*, *33*, 297–303. https://doi.org/10.3189/172756401781818338

Tremblay, J. É., Bélanger, S., Barber, D. G., Asplin, M., Martin, J., Darnis, G., et al. (2011). Climate forcing multiplies biological productivity in the coastal Arctic Ocean. *Geophysical Research Letters*, *38*(18), L18604. https://doi.org/10.1029/2011GL048825

Ulfsbo, A., Cassar, N., Korhonen, M., Van Heuven, S., Hoppema, M., Kattner, G., & Anderson, L. G. (2014). Late summer net community production in the central Arctic Ocean using multiple approaches. *Global Biogeochemical Cycles*, *28*(10), 1129–1148. https://doi.org/10.1002/2014GB004833

Venables, H., & Moore, C. M. (2010). Phytoplankton and light limitation in the Southern Ocean: Learning from high-nutrient, high-chlorophyll areas. *Journal of Geophysical Research*, *115*(C2), C02015. https://doi.org/10.1029/2009JC005361

Walker, S. A., Amon, R. M. W., & Stedmon, C. A. (2013). Variations in high-latitude riverine fluorescent dissolved organic matter: A comparison of large arctic rivers. *Journal of Geophysical Research: Biogeosciences*, *118*(4), 1689–1702. https://doi.org/10.1002/2013JG002320

Watanabe, E., Onodera, J., Itoh, M., Nishino, S., & Kikuchi, T. (2017). Winter transport of subsurface warm water toward the Arctic Chukchi Borderland. *Deep-Sea Research Part I*, *128*, 115–130. https://doi.org/10.1016/j.dsr.2017.08.009

Wheeler, P. A., Watkins, J. M., & Hansing, R. L. (1997). Nutrients, organic carbon and organic nitrogen in the upper water column of the Arctic Ocean: Implications for the sources of dissolved organic carbon. *Deep-Sea Research Part II*, *44*(8), 1571–1592. https://doi.org/10.1016/S0967-0645(97)00051-9

Wickland, K. P., Aiken, G. R., Butler, K., Dornblaser, M. M., Spencer, R. G. M., & Striegl, R. G. (2012). Biodegradability of dissolved organic carbon in the Yukon River and its tributaries: Seasonality and importance of inorganic nitrogen. *Global Biogeochemical Cycles*, *26*(4), GB0E03. https://doi.org/10.1029/2012GB004342

Woodgate, R. A., & Aagaard, K. (2005). Revising the Bering Strait freshwater flux into the Arctic Ocean. *Geophysical Research Letters*, *32*(2), L02602. https://doi.org/10.1029/2004GL021747

Yamamoto-Kawai, M., McLaughlin, F. A., Carmack, E. C., Nishino, S., & Shimada, K. (2008). Freshwater budget of the Canada Basin, Arctic Ocean, from salinity, $\delta^{18}O$, and nutrients. *Journal of Geophysical Research*, *113*(C1), C01007. https://doi.org/10.1029/2006JC003858

Yamamoto-Kawai, M., McLaughlin, F. A., Carmack, E. C., Nishino, S., Shimada, K., & Kurita, N. (2009). Surface freshening of the Canada Basin, 2003–2007: River runoff versus sea ice meltwater. *Journal of Geophysical Research*, *114*, C00A05. https://doi.org/10.1029/2008JC005000

Yamamoto-Kawai, M., Tanaka, N., & Pivovarov, S. (2005). Freshwater and brine behaviors in the Arctic Ocean deduced from historical data of $\delta^{18}O$ and alkalinity (1929–2002 A.D.). *Journal of Geophysical Research*, *110*(C10), C10003. https://doi.org/10.1029/2004JC002793

Zhang, C., Dang, H., Azam, F., Benner, R., Legendre, L., Passow, U., et al. (2018). Evolving paradigms in biological carbon cycling in the ocean. *National Science Review*, *5*(4), 481–499. https://doi.org/10.1093/nsr/nwy074

Zhang, J., Spitz, Y. H., Steele, M., Ashjian, C., Campbell, R., & Schweiger, A. (2020). Biophysical consequences of a relaxing Beaufort Gyre. *Geophysical Research Letters*, *47*(2), e2019GL085990. https://doi.org/10.1029/2019GL085990